



DNA 5050F

# THERMAL TESTING OF ADVANCED MISSILE MATERIALS

12

Los Alamos Technical Associates, Inc  
P.O. Box 410  
Los Alamos, New Mexico 87544

LEVEL II

31 August 1979

Final Report for Period 1 March 1979—31 August 1979

CONTRACT No. DNA 001-79-C-0234

APPROVED FOR PUBLIC RELEASE;  
DISTRIBUTION UNLIMITED.

DTIC  
SELECTE  
JUL 31 1981  
S D  
E

THIS WORK SPONSORED BY THE DEFENSE NUCLEAR AGENCY  
UNDER RDT&E RMSS CODE B342079464 N99QAXAK11212 H2590D.

Prepared for  
Director  
DEFENSE NUCLEAR AGENCY  
Washington, D. C. 20305

AD A102253

DTIC FILE COPY

81 8 29 008

Destroy this report when it is no longer needed. Do not return to sender.

PLEASE NOTIFY THE DEFENSE NUCLEAR AGENCY,  
ATTN: STTI, WASHINGTON, D.C. 20305, IF  
YOUR ADDRESS IS INCORRECT, IF YOU WISH TO  
BE DELETED FROM THE DISTRIBUTION LIST, OR  
IF THE ADDRESSEE IS NO LONGER EMPLOYED BY  
YOUR ORGANIZATION.



UNCLASSIFIED

SECURITY CLASSIFICATION OF THIS PAGE (When Data Entered)

REPORT DOCUMENTATION PAGE		READ INSTRUCTIONS BEFORE COMPLETING FORM
1 REPORT NUMBER <b>18</b> DNA 5050P <b>19</b>	2 GOVT ACCESSION NO AD-A202 253	3 RECIPIENT'S CATALOG NUMBER
4 TITLE (and Subtitle)  THERMAL TESTING OF ADVANCED MISSILE MATERIALS		5 TYPE OF REPORT & PERIOD COVERED Final Report for Period 3/1/79 - 8/31/79
7 AUTHOR(s)  John C. Kimerly <del>and</del> Peter S. Hughes		6 PERFORMING ORG. REPORT NUMBER <b>14</b> LATA-715 CONTRACT OR GRANT NUMBER  <b>15</b> DNA 001-79-C-0234 <i>new</i>
8 PERFORMING ORGANIZATION NAME AND ADDRESS Los Alamos Technical Associates, Inc. P. O. Box 410 Los Alamos, New Mexico 87544		10 PROGRAM ELEMENT PROJECT TASK AREA & WORK UNIT NUMBERS <b>16</b> <b>17</b> Subtask N99QAXAK112-12
11 CONTROLLING OFFICE NAME AND ADDRESS Director Defense Nuclear Agency Washington, D.C. 20305		12 REPORT DATE <b>11</b> 31 August 1979
14 MONITORING AGENCY NAME & ADDRESS, if different from Controlling Office <b>9</b> Final Rept. 4 Mar-31 Aug 79		13 NUMBER OF PAGES 72
		15 SECURITY CLASS. of this report UNCLASSIFIED
16 DISTRIBUTION STATEMENT of this Report  Approved for public release; distribution unlimited.		15a DECLASSIFICATION/DOWNGRADING SCHEDULE
17 DISTRIBUTION STATEMENT of the abstract entered in Block 20, if different from Report		
18 SUPPLEMENTARY NOTES  This work sponsored by the Defense Nuclear Agency under RDT&E RMSS Code B342079464 N99QAXAK11212 H2590D.		
19 KEY WORDS (Continue on reverse side if necessary and identify by block number) Thermal Radiation      Advanced Missile Nuclear Thermal      External Protection Materials (EPM) Ablation      Test Facilities Pyrometry      Material Response to Thermal Radiation		
20 ABSTRACT (Continue on reverse side if necessary and identify by block number)  This report documents an experimental program for the exposure of external protection material (EPM) candidates to simulated nuclear thermal radiation. A draft test spec was developed and applicable test facilities were surveyed. Experiments were conducted at the Tri-Service Thermal Flash Test Facility at Wright-Patterson AFB to (1) characterize the convective cooling coefficient of the quartz lamp/wind tunnel test		

427897

UNCLASSIFIED

SECURITY CLASSIFICATION OF THIS PAGE(When Data Entered)

section, (2) develop front surface pyrometry and thermocouple techniques to accurately measure the ablative surface temperature, and (3) test a variety of EPM candidates to thermal flash environments.

The conclusions reached in this project are that the Tri-Service Thermal Flash Test Facility at Wright-Patterson AFB is the most applicable facility for screening tests of EPM candidates. Front surface temperature measurements are needed to accurately model the ablation and thermal deposition characteristics. Continued testing is needed for full scale engineering development of the EPM and for quality assurance during production of the advanced missile system.

UNCLASSIFIED

SECURITY CLASSIFICATION OF THIS PAGE(When Data Entered)

SUMMARY

The primary purpose of the "Thermal Testing of Advanced Missile External Protection Materials" was to provide a responsive engineering service to the DNA sponsor and to those involved in development of the advanced strategic missiles to help evaluate the response of proposed external protection materials (EPM) to simulated nuclear thermal flash.

Three tasks were performed by Los Alamos Technical Associates, Inc. (LATA). The first resulted in an accurate measurement of the convective cooling coefficient of the Tri-Service Thermal Radiation Facility's wind tunnel. The second developed a front-surface pyrometer for use in EPM evaluation using the same wind tunnel.

The third task consisted of leading a team composed of TRW, McDonnell Douglas, University of Dayton Research Institute (UDRI) and LATA personnel in a program at the Tri-Service Thermal Radiation Facility in which 31 highly instrumented EPM specimens were tested.

In addition to the test programs, LATA completed a survey of the engineering community to identify potential thermal flash testing facilities. A listing of these facilities is included in this report. (Table 1)

A preliminary draft of a thermal flash testing method/specification is appended for coordination by the advanced strategic missile community.

Accession For	
NTIS GRA&I	<input checked="" type="checkbox"/>
DTIC TAB	<input type="checkbox"/>
Unannounced	<input type="checkbox"/>
Justification	<input type="checkbox"/>
By _____	
Distribution/	
Availability Codes	
Dist	Avail and/or Special
<b>A</b>	

## PREFACE

This report describes a program to standardize thermal test techniques to evaluate the nuclear thermal flash response to external protection materials (EPM) for strategic missile applications.

This work was funded by the Defense Nuclear Agency under contract number DNA001-79-C-0234. The contracting officer representative was Capt. A. T. Hopkins. The period of performance was from March 1, 1979 to August 31, 1979.

The authors would like to acknowledge the support and assistance of the personnel of the Tri-Service Thermal Radiation Test Facility at Wright-Patterson Air Force Base, Dayton, Ohio.

CONVERSION FACTORS  
TO S.I. UNITS

<u>To Convert From</u>	<u>To</u>	<u>Multiply By</u>
pounds per square inch	newtons per square centimeter	0.689
gram calorie	Joules	4.185
British Thermal Unit	Joules	1.055
Inches	Centimeters	2.54
Feet	Meters	0.3048

$$(^{\circ}\text{F}-32) \times 5/9 + 273 = ^{\circ}\text{K}$$

$$^{\circ}\text{C} + 273 = ^{\circ}\text{K}$$



## TABLE OF CONTENTS

	<u>Page</u>
SUMMARY	1
PREFACE	2
CONVERSION FACTORS TO S.I. UNITS	3
LIST OF ILLUSTRATIONS	5
1.0 INTRODUCTION	7
1.1 Background	7
1.2 Project Objectives	7
2.0 PRIMARY PROJECT RESULTS	9
2.1 Overview of Project	9
2.2 Convective Cooling Coefficient Experiments	10
2.3 Front Surface Pyrometry Experiments	10
2.4 Survey of Nuclear Thermal Test Facilities	10
2.5 Draft Thermal Flash Testing Specification	13
2.6 Thermal Screening Tests of EPM Specimens	13
3.0 CONCLUSIONS	14
4.0 RECOMMENDATIONS	16
 <u>APPENDIX</u>	
A MEASUREMENT OF THE CONVECTIVE COOLING COEFFICIENT OF THE TRI-SERVICES THERMAL RADIATION FACILITY WIND TUNNEL BY MEANS OF A GUARDED HOT PLATE	A-1
B FRONT SURFACE TEMPERATURE MEASUREMENT FOR ABLATING MATERIALS BY SURFACE PYROMETRY	B-1
C PROPOSED TEST METHOD FOR EVALUATING THE THERMAL FLASH RESPONSE OF EXTERNAL PROTECTION MATERIALS BY UTILIZING UTILIZING A QUARTZ-TUNGSTEN LAMP THERMAL SOURCE	C-1

LIST OF ILLUSTRATIONS

<u>Figure</u>		<u>Page</u>
A-1	Wind tunnel schematic - - - - -	A-3
A-2	Guarded hot plate - - - - -	A-5
A-3	Convective cooling as a function of surface temperature 70°F and 75°F static temperatures - - - - -	A-8
A-4	Convective cooling as a function of air speed and surface temperature - - - - -	A-9
B-1	Specimen configuration - - - - -	B-11
B-2	Transmittance of quartz and emission of a 3000°K tungsten filament - - - - -	B-12
B-3	6.8 micron cut-on filter transmittance - - - - -	B-13
B-4	Pyrometer positioned in wind tunnel - - - - -	B-14
B-5	Pyrometer calibration curve - - - - -	B-15
B-6	Infrared reflectance of test material - - - - -	B-16
B-7	Run #6251, VAMAC 25 exposed to 30 cal/cm <sup>2</sup> /sec for 3 sec - - - - -	B-17
B-8	Run #6252, Specimen #1 of VAMAC 151B, exposed to 30 cal/cm <sup>2</sup> /sec for 3 sec - - - - -	B-18
B-9	Run #6253, Specimen #2, VAMAC 151B exposed to 30 cal/cm <sup>2</sup> /sec for 3 sec - - - - -	B-19
B-10	Run #6254, VAMAC 151A, Specimen #1, exposed for 3 sec at 30 cal/cm <sup>2</sup> /sec - - - - -	B-20
B-11	Run #6255, VAMAC 151A, Specimen #2, exposed to 30 cal/cm <sup>2</sup> /sec for 3 sec - - - - -	B-21
B-12	Run #6256, Royacril exposed to 30 cal/cm <sup>2</sup> /sec for 3 sec - - - - -	B-22
B-13	Run #6257, VAMAC 151A with subsurface thermo- couple, first test 30 cal/cm <sup>2</sup> /sec for 3 sec - - - - -	B-23
B-14	Run #6258, VAMAC 151A with subsurface thermo- couple, first retest 30 cal/cm <sup>2</sup> /sec for 3 sec - - - - -	B-24

LIST OF ILLUSTRATIONS (Concluded)

<u>Figure</u>		<u>Page</u>
B-15	Run #6259, VAMAC 151A with subsurface thermo- couple, second retest 30 cal/cm <sup>2</sup> /sec for 3 sec - - - - -	B-25
B-16	Run #6260, VAMAC 151A with subsurface thermo- couple, third retest 30 cal/cm <sup>2</sup> /sec for 3 sec - - - - -	B-26
B-17	Run #6261, VAMAC 151B with subsurface thermo- couple, first test, 30 cal/cm <sup>2</sup> /sec for 3 sec - - - - -	B-27
B-18	Run #6262, VAMAC 151B with subsurface thermo- couple, first retest 30 cal/cm <sup>2</sup> /sec for 3 sec - - - - -	B-28
B-19	Run #6263, VAMAC 151B with subsurface thermo- couple, second retest 30 cal/cm <sup>2</sup> for 3 sec - - - - -	B-29
C-1	Suitable thermal flash testing facility - - - - -	C-4
C-2	Typical test specimen configuration - - - - -	C-5
C-3	Suitable slug calorimeter design - - - - -	C-8

## 1.0 INTRODUCTION

### 1.1 BACKGROUND

The technical effort covered in this report was initially proposed by the Los Alamos Technical Associates, Inc. (LATA) to the Defense Nuclear Agency (DNA) in an unsolicited proposal and was eventually funded under Contract DNA001-79-C-0234. This effort was primarily intended to support DNA's advanced technology program to develop external protection materials (EPM). A variety of external coatings were being proposed to protect the shroud and the four missile stages from the various environments encountered during fly-out flight phase. The DNA advanced technology program was exploring several alternative EPM materials. LATA's participation was to provide for an impartial, unbiased, carefully designed and documented experimental program to evaluate the thermal protection qualities of a variety of candidate materials. These materials were supplied by the DNA specified contractors.

The work on this project began March 1, 1979, with the initial effort being an investigation of available nuclear thermal radiation simulation facilities.

### 1.2 PROJECT OBJECTIVES

In support of the EPM development for MX, LATA served as impartial, independent thermal test coordinator and conductor for DNA (SPAS). Specific objectives of this project were:

- review the draft Thompson-Ramo-Wooldridge and Space and Missile Systems Organization (TRW) and (SAMSO) coordinated specifications for the nuclear thermal radiation fly-out environment. In addition, LATA was to attend specification coordination meetings and to draft a thermal flash testing specification for the EPM candidates;

- design a testing program to expose EPM specimens (supplied by various DNA and SAMS0 contractors) to simulated nuclear thermal radiation at an appropriate test facility;
- develop a consistent test specimen configuration and thermocouple instrumentation procedure;
- survey the existing thermal flash test facilities and compare their applicability to the program requirements;
- take the test specimens to the selected thermal flash test facility and supervise the recording of the incident thermal exposure and the specimen's back-face temperature transient; and
- serve as an advisor concerning the applicability of EPM and thermal test techniques.

## 2.0 PRIMARY PROJECT RESULTS

### 2.1 OVERVIEW OF PROJECT

During the performance of the contract, the following principal efforts were expended:

- LATA personnel accurately determined the convective cooling coefficient of the wind tunnel at the Tri-Service Thermal Radiation Facility at Wright Patterson AFB;<sup>1,2</sup>
- LATA personnel developed a front-surface pyrometer for measuring front surface temperatures of samples tested in the Tri-Service Thermal Radiation Facility;
- the engineering community was surveyed to locate, identify, and evaluate potential thermal testing facilities;
- a thermal testing specification was drafted and readied for coordination; and
- engineering support was provided to test a series of highly instrumented specimens at the Tri-Service Thermal Radiation Facility.

- 
1. Servias, R. A., Wilt, B. H., and Olson, N. J., "Tri-Service Thermal Flash Test Facility," Defense Nuclear Agency, Washington, D.C., DNA 4757F (November 30, 1978).
  2. Servias, R. A., Wilt, B. H., and Olson, N. J., "Tri-Service Thermal Radiation Test Facility: Test Procedures Handbook," University of Dayton Research Institute, Dayton, Ohio, UDRI-TR-77-28 (May 1977).

## 2.2 CONVECTIVE COOLING COEFFICIENT EXPERIMENTS

The need for accurate convective cooling coefficient data arose when efforts were made to try to match experimental data taken from and computer modeling of the Tri-Service Thermal Radiation Facility . The energy equation could not be made to balance with the previously determined values of the convective cooling coefficient.<sup>1</sup> A LATA designed and conducted experiment established a value approximately 50% of the previously used value. The test method and results are given in Appendix A.

## 2.3 FRONT SURFACE PYROMETRY EXPERIMENTS

Configurational problems make it nearly impossible to continuously monitor with thermocouples the front surface temperature of ablating EPMs. However, it was deemed necessary to determine these front-surface temperatures to complete the thermal model of ablating EPMs. Optical pyrometry was used for this determination. Appendix B describes a test method and equipment used by LATA to accomplish the necessary pyrometry. Significantly higher temperatures were observed than had been previously recorded by the more rudimentary thermocouple techniques.

## 2.4 SURVEY OF NUCLEAR THERMAL SIMULATION TEST FACILITIES

In an attempt to identify those facilities best capable of simulating the required thermal flash environment, LATA conducted a nationwide survey of thermal flash facilities. Table 1 is presented as a summary of those facilities. It is not an exhaustive list; it is intended to present one or two choices of each of the major types of thermal sources.

- 
1. Fazekas, F. S. (Captain USAF), "An Analysis of the Tri-Service Thermal Radiation Test Facility," Air Force Institute of Technology Master's Thesis, Wright-Patterson AFB, Ohio, AFIT-GAE-AA-77D-4 (December 1977).

TASK 1. TEST FACILITIES

Type	Location	Source "Temperature °K	Q <sub>max</sub> cal/cm <sup>2</sup> /sec	Air Flow ft/s	Pulse Shaping	Exposure Area	Exposure Uniformity	Usage Cost *	Comments
Quartz/ Tungsten Lamp Banks	Rockwell, Inc. Los Angeles Division El Segundo, CA	3650	70	150 ft/s	Very Good	10 cm x 15 cm	Good	No quote	Highest peak flux for this type facility.
	Tri-Services Thermal Radiation Test Facility W.P. AFB, Dayton, OH	3500	55	740 ft/s	Good	7.5 cm x 12.7 cm	Fair	Virtually none sup- ported by DNA.	Highest peak flux for this type facility.
Solar Furnace	Sandia Solar Thermal Test Facility, Sandia Laboratories Albuquerque, NM	6000	50	None	No capability at present.	1M Dia	Gaussian	~\$12,000/wk	
	Georgia Tech 400 KW ACTF, Georgia Tech	6000	50	None	No capability.	.5 + 1 meter	Irregular	No quote.	Not easily accessible for materials testing.
	White Sands Solar Furnace White Sands Missile Range, NM	6000	100	740 ft/s	Very Good	12.7 cm - Dia.	Gaussian	Available to Gov't con- tracts only.	Test Facility is remote
	CNRS Solar Facility Odeillo, France	6000	380	None	User provides own.	1 meter	Gaussian	Very High	User must supply all support equipment.
Plasma Jets	Tri-Services Thermal Radiation Test Facility, WPAFB	5,000*	Very High	None	No capability	2.45 cm	Poor	Virtually none, DNA supported	Not operable at present.
	Rockwell International Space Division, Downey, CA	5,000	Very High	None	No capability.	2.54 Dia.	Poor	No quote.	Used for rocket plume impingement test.
Lasers	NASA Ames Moffet Field, CA	10.6 micron Monochromatic	~300	mach 1.4	Good	>2 cm Dia.	Very Poor	No quote.	Very versatile test facility, wind perpen- dicular to test area.
	AVCO Everett, MA	10.6 micron Monochromatic	~300	None	Good	>2 cm Dia.	Very Poor	\$1,250/day	

\* Estimate Only



TABLE 1. TEST FACILITIES  
(Continued)

Type	Location	Source Temperature °K	Q <sub>max</sub> cal/cm <sup>2</sup> /sec	Air Flow	Pulse Shaping	Exposure Area	Exposure Uniformity	Usage Cost *	Comments
Xenon Pinched ARC Furnace	NASA AMES Moffet Field, CA	No data available							Not in current use
ARC Imaging Furnaces	Tri-Services Thermal Radiation Test Facility, WPAFB	6,000	140	None	Fair	2.0 cm Dia.	Gaussian	0	
Graphite	Rockwell International Los Angeles Division	2,000	20	None	Fair	60 cm x 60 cm	Very Uniform	Varies	Very low black-body temperature.
Chemical Explosions	Naval Surface Weapons Center, White Oak Laboratory Silver Spring, MD	Not in service at present							Rocket pro- pellant burn; combustion products very corrosive.
Flash Bags	DNA Thermal Radiation Facility, Kirtland AFB, NH	3,000	65	No	Fair	Unlimited	Good	Very High	Aluminum/ Oxygen burn, quasi-nuclear pulse con- trolled by mixing rates.
ARC Heated Wind Tunnel	NASA Ames Moffet Field, CA	Not applicable, convective heating	40	mach >1	No	15 cm x 15 cm	Fair	No quote.	Excellent "second" approach to ablation studies.

\* Estimate only

## 2.5 DRAFT THERMAL FLASH TESTING SPECIFICATION

A preliminary draft of a thermal flash testing specification is presented in Appendix C. The purpose of this specification is to provide a standard test method which will produce repeatable results and permit comparison materials on a consistent basis.

The specification provides three levels of test. The first is intended to generate thermal transport data below the material's ablation temperature. The second, using a very simple square wave pulse, is to be used to identify ablation processes. This type of pulse is far more amenable to initial analyses than is a tailored pulse. The third level pulse is intended to reproduce the net thermal flux through the surface of the EPM as predicted by mission profile analysis. This test is intended primarily as a check of the resultant final computer models and possibly as a receiving inspection or qualification type test. However, depending upon the mission profile, this type of pulse may not be producible in the laboratory test facilities.

## 2.6 THERMAL SCREENING TESTS OF EPM SPECIMENS

On July 16, 1979, LATA personnel traveled to the Air Force Materials Lab (AFML), Dayton, Ohio, to assist in a series of thermal tests on EPMs using the Tri-Service Thermal Radiation Facility. In attendance were P. Spangler, McDonnell-Douglas; D. Hender, McDonnell-Douglas; B. Bacharach, TRW; J. Kimerly, LATA; and N. Olsen, UDRI.

A total of 31 specimens of various types of EPMs were tested, most with five imbedded thermocouples, and all utilizing front-surface pyrometry. The resultant data are in the process of being analyzed by McDonnell-Douglas and TRW representatives. A preliminary report of the results are contained in McDonnell-Douglas Seventh Monthly Progress Letter, "Advanced Booster Hardening Technology Program," dated August 1979.

These data are the most complete of any gathered to date, and should result in satisfactory thermal transport modeling.

### 3.0 CONCLUSIONS

(1) The convective cooling coefficient previously reported for the Tri-Service Thermal Radiation Facility was high by about 125 percent. Through a carefully controlled experiment, a value of about  $44.0 \text{ Btu/ft}^2/\text{hr}/\text{F}^\circ$  was determined. This should significantly affect the mathematical modeling of the heat transfer process of the EPM specimens.

(2) Bayonet thermocouple techniques are not adequate for measuring transient temperatures of ablative EPMs. This is particularly true when trying to determine the front-surface and ablative characteristics.

(3) The actual EPM front-surface temperatures are significantly more variable than expected. The optical pyrometry technique developed by Mr. Kimerly demonstrated this fact. This is most likely a result of complex processes associated with the initial formation of a char layer and the stability of that fragile layer. For example, at the onset of ablation, the polymer binder exists as a high molecular weight hydrocarbon with good thermal stability. As this chain is thermally scissioned, two products appear. These are a low-density carbonaceous solid, and lower molecular weight polymers, possibly free radicals. These lower molecular weight types can be expected to exhibit ablation temperatures different from the base polymer. If they should spall off, the temperature would revert to the base polymer break-down temperature.

(4) In the course of this contract, it became apparent that no existing thermal flash facility can totally duplicate the desired thermal flash test environment in terms of ambient pressure, supersonic airflow, thermal flux, and thermal spectrum. However, many of them can be used to derive thermal response data that can be used to calibrate computer thermal codes. The Tri-Service Thermal Radiation Facility is suitable for testing opaque materials. The solar furnace at White Sands Missile Range is the best facility available for the testing of transparent materials.

(5) A specification for thermal flash testing has been developed. (See App. C).

(6) The screening tests conducted this far have yielded a considerable quantity of valuable data that can be used to derive ablative models for the primary EPM candidates.

#### 4.0 RECOMMENDATIONS

(1) The thermocouples used to determine the heat transfer through the EPM specimens should be small diameter ( $\leq 5$  mil) and should follow isothermal installation practices.

(2) An adequate test facility exists in the Tri-Service Thermal Flash Facility. It is cost-effective and reasonably complete. It is recommended this facility be used to (a) screen further EPM candidates, and (b) derive data to build and verify predictive thermal computer codes for the EPM candidates. Once a sufficient thermal model is constructed for each candidate EPM, thermal response can be computed for any combination of flight profiles and thermal exposures.

(3) A common thermal analysis code should be developed to support the test specification. Such a code would facilitate comparison of test data between different tests series, users, and test conditions.

(4) Test facilities should be further investigated and test procedures should be developed for (a) tests of full scale and production EPM systems on appropriate substrates, and (b) qualification tests of production missile stages and/or the entire missile.

APPENDIX A  
MEASUREMENT OF THE CONVECTIVE COOLING COEFFICIENT  
OF THE  
TRI-SERVICES THERMAL RADIATION FACILITY WIND TUNNEL  
BY MEANS OF A GUARDED HOT PLATE

A.1.0 INTRODUCTION

The University of Dayton Research Institute operates a nuclear thermal flash simulation facility under contract to the Defense Nuclear Agency. This facility is located at Wright-Patterson Air Force Base, Dayton, Ohio.

The facility consists of a quartz-tungsten high-energy lamp bank, a subsonic wind tunnel, and peripheral support equipment. This report describes a test method and equipment that were developed for measuring the aerodynamic convective cooling coefficient of this wind tunnel and the data resultant from the use of this test equipment. The test method described is a derivative of the guarded hot plate test method of ASTM-C-177-71.<sup>1</sup>

A.2.0 BACKGROUND

The Tri-Service Thermal Radiation Facility is currently being used by various government agencies and government contractors to evaluate the response of various coatings, structures, and external protection materials to intense thermal radiation such as might be encountered by exposure to the environment created by nuclear weapons detonations. UDRI-TR-77-28, "Tri-Service Thermal Radiation Test Facility: Test Procedures Handbook,"<sup>2</sup> describes, in general, the operation and capabilities of this facility. A more detailed analysis of the physical characteristics of the facility is presented in AFIT/GAE/AA/77D-4, "An Analysis of the Tri-Service Thermal Radiation Test."<sup>3</sup> Section IV of that report describes a method used to determine the convective heat transfer coefficient of the wind tunnel used in conjunction with the thermal source.

Attempts to correlate EPM test results with computer modeling have been inconsistent and generally unsuccessful. In addition, the procedures originally used to determine the wind tunnel convective heat transfer coefficient were suspect. These erroneous results could have been a source of error in the computer modeling. An alternate method was then devised and used to remeasure the convective heat transfer coefficient of the wind tunnel.

The method initially used to determine the convective heat transfer coefficient consisted essentially of irradiating a copper slug calorimeter with the quartz-tungsten lamp bank with and without the wind tunnel in operation (see Figure A-1). A reasonably valid assumption was made that the radiative and conductive losses to the environment were negligible during the test. The heat balance equation then becomes

$$\alpha I = \text{storage} + q \text{ conv} = \rho c t \frac{dT_c}{dt} + h (T_c - T_a) \quad (\text{A-1})$$

where

- $I$  = incident thermal flux,
- $\alpha$  = absorbtivity of the copper slug to the incident thermal flux,
- $\rho$  = density of copper,
- $c$  = specific heat of copper,
- $t$  = thickness of the copper slug,
- $\frac{dT_c}{dt}$  = time rate of change of temperature of the copper slug,
- $h$  = convective heat transfer coefficient (taken to be zero with no air flow),
- $T_c$  = temperature of the copper slug, and
- $T_a$  = temperature of the wind tunnel air.

With the wind tunnel off, the second term of the equation becomes zero, and  $\alpha$  was determined assuming  $I$  was known. (At the time of these tests,  $I$  was probably determinable to no better than  $\pm 10\%$ .)

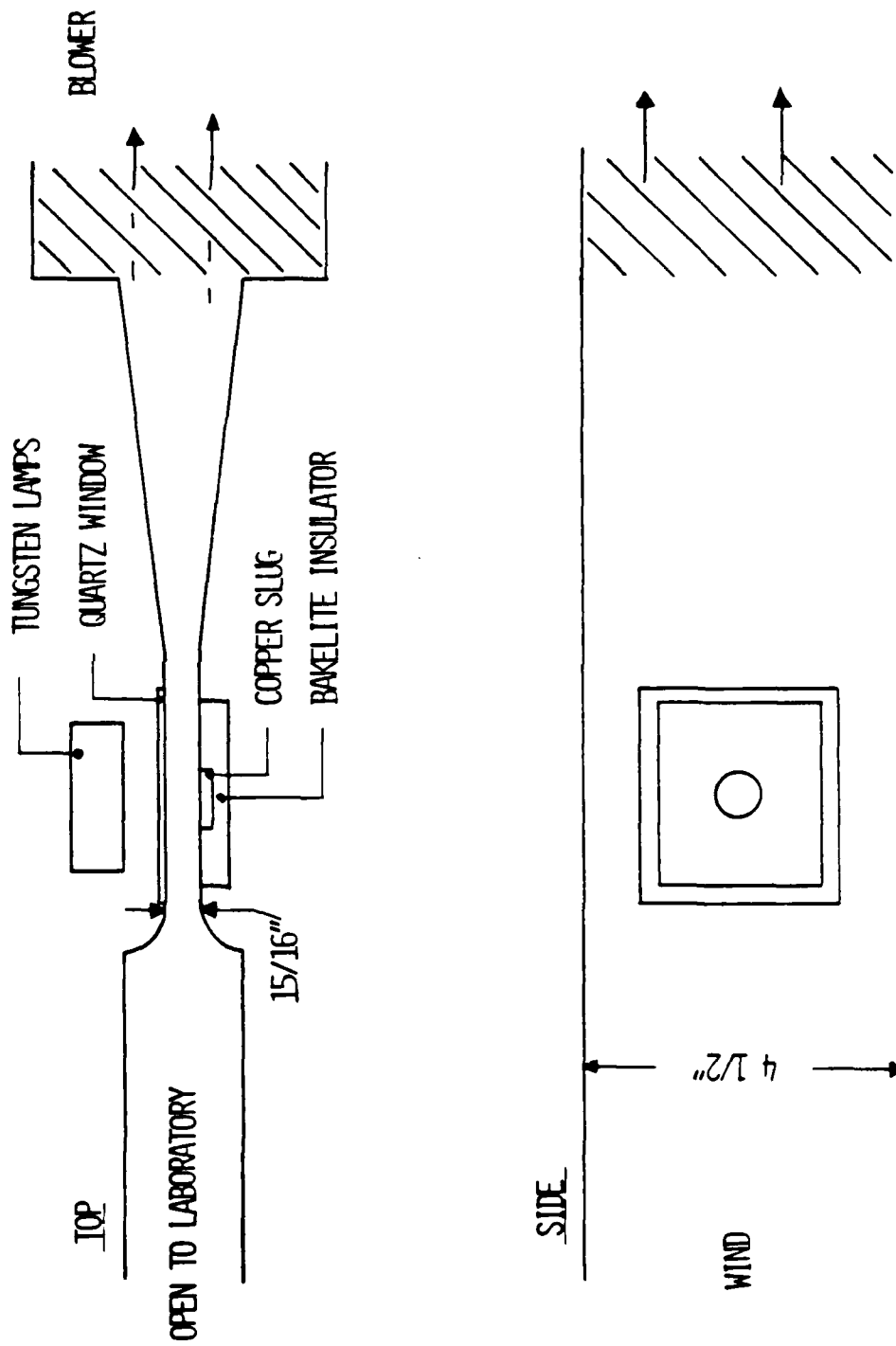


Fig. A-1 Wind tunnel schematic.



The procedure was then repeated with air flow;  $h$  could then be determined. Using these procedures,  $\alpha$  was determined to be 0.2189 for bare copper. That is a very high value for copper exposed to a 2,700 K source.  $T_a$  was taken as 116°F (320 K). For a tunnel of this design and with the heated flow length concerned, it should have been the adiabatic wall temperature, or something close to ambient temperature. By this procedure,  $h$  was determined to be 100 Btu ft<sup>-2</sup> hr<sup>-1</sup> f<sup>-1</sup>.

Because of the previously stated concerns, it was described that a method was needed to determine  $h$  that did not require knowledge of  $I$ ,  $\alpha$ , or the effective  $T_a$  of the wind tunnel. The method selected was a guarded hot plate method.

#### A.3.0 THE GUARDED HOT PLATE TEST METHOD

Figure A-2 is a schematic drawing of the guarded hot plate. In concept, measured electrical power is applied to the main heater. The ring guard and back guard are adjusted so that no heat flow occurs between them and the main heater as by measured thermocouples and heat flux meters. All power to the main heater is, therefore, dissipated into the windstream. The surface temperature of the main heater is monitored. All measurements are taken at equilibrium conditions. A plot can then be made of the power per square unit area dissipated by the heater versus the heater surface temperature. The slope of this plot is  $h$ .

The air speed was computed by

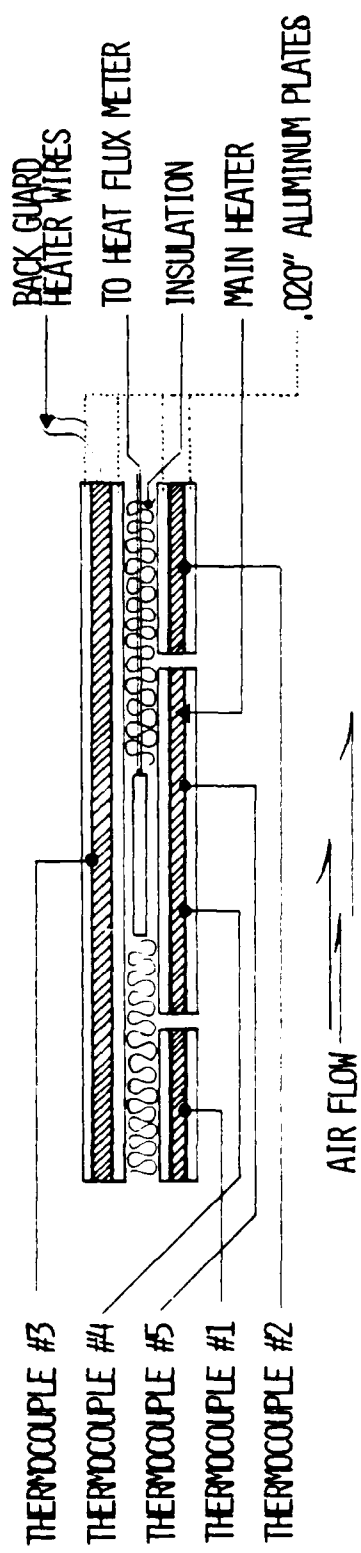
$$V = \sqrt{\frac{2\Delta p}{\rho_a}} \quad (\text{A-2})$$

where

$V$  is in feet per second,

$\Delta p$  is the difference between the pitot and static pressure, and

$\rho_a$  is the air density at the given static pressure.



AIR FLOW →

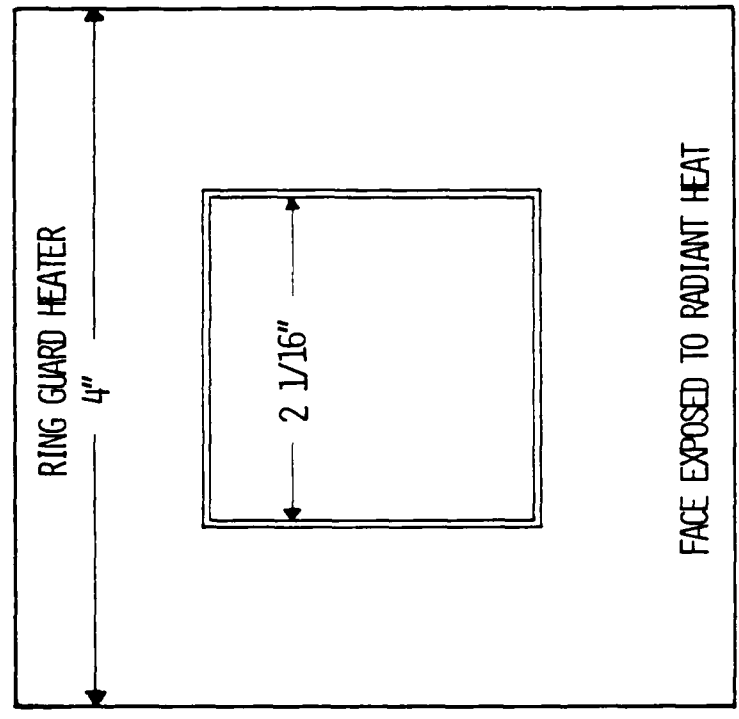


Fig. A-2 Guarded hot plate.

#### A.4.0 RESULTS

Convective cooling coefficient data were taken on three consecutive days. The raw data are listed in Table A-1. Figure A-3 is a plot of the results of the first two days. The top line was the result of the first day's test. Ambient temperature was 70° F. The lower line was the result of the second day when the ambient temperature was 75° F. Both were taken at the maximum possible air speed of the wind tunnel. In each case, thermocouple No. 4 is shown on the left, thermocouple No. 5 on the right, and the arrow indicator the intercept of the applicable line. Figure A-4 illustrates the results of varying air speed. The top curve is a retrace of the top curve in Figure A-3. The central curve is a result of partial venting the wind tunnel downstream of the test section. The lower curve is a result of even more venting. The point labeled A on the upper curve represents data taken with a shutter in place in the middle of the air stream for purposes of blocking the view of the lamps from the test sample.

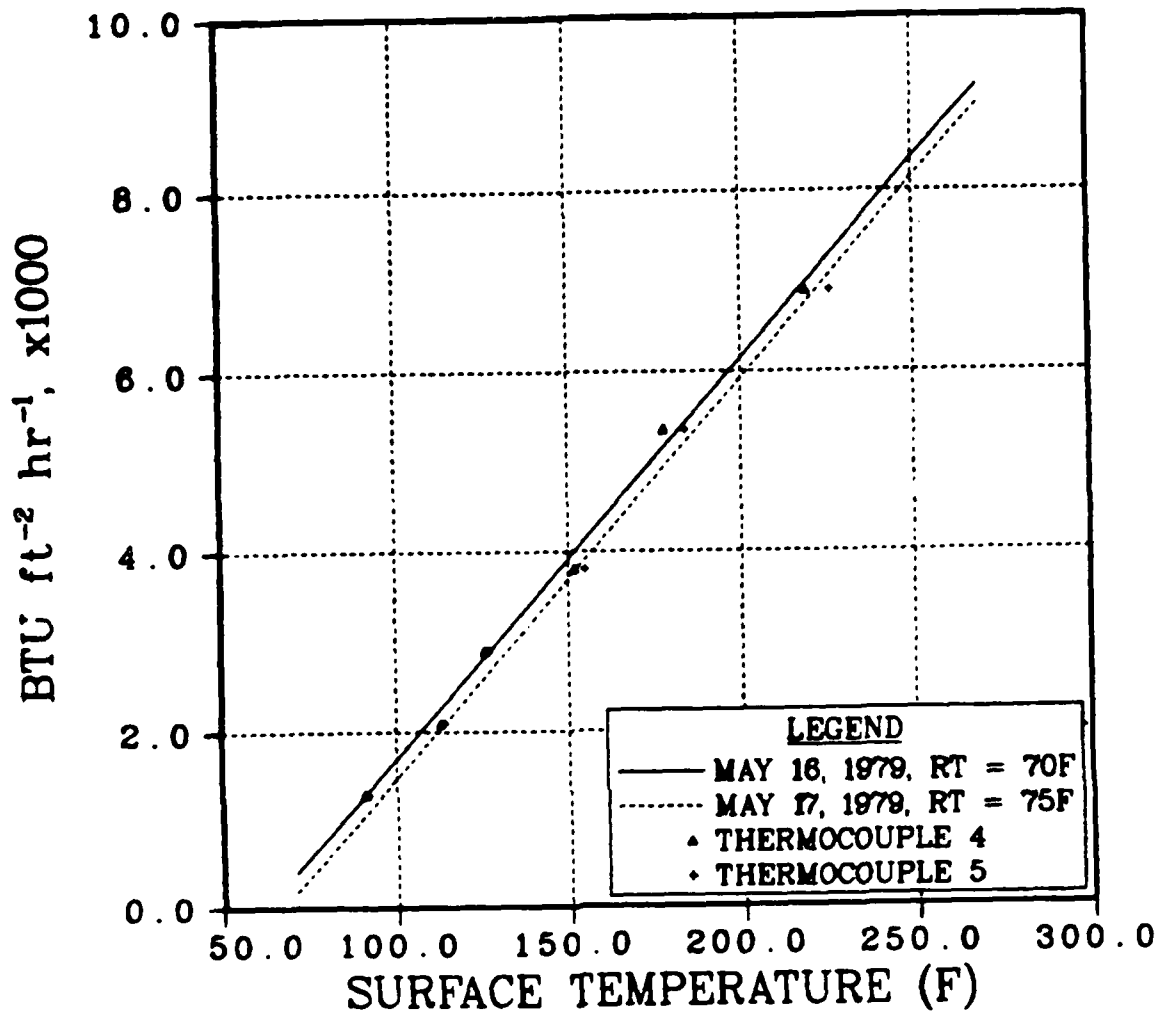
Since it was obvious that the shutter had minimal effect, no other data were taken with it in place.

These data result in an  $h$  of  $44.0 \text{ Btu ft}^{-2} \text{ hr}^{-1} \text{ }^{\circ}\text{F}^{-1}$  as compared to the previously reported values of  $100 \text{ Btu ft}^{-2} \text{ hr}^{-1} \text{ }^{\circ}\text{F}^{-1}$  at maximum air speed. They also indicated that  $h$  is a very loose function of air speed. The measured value of  $44.0 \text{ Btu ft}^{-2} \text{ hr}^{-1} \text{ }^{\circ}\text{F}^{-1}$  is certainly below that value that might be computed by classical text book methods. This is apparently the result of a highly complex flow pattern within the test section of the wind tunnel. It can be expected that the blow-off effects during ablation of a test specimen will further "trip" the flow pattern and lower the local convective cooling.

TABLE A-1  
WIND TUNNEL TEST DATA

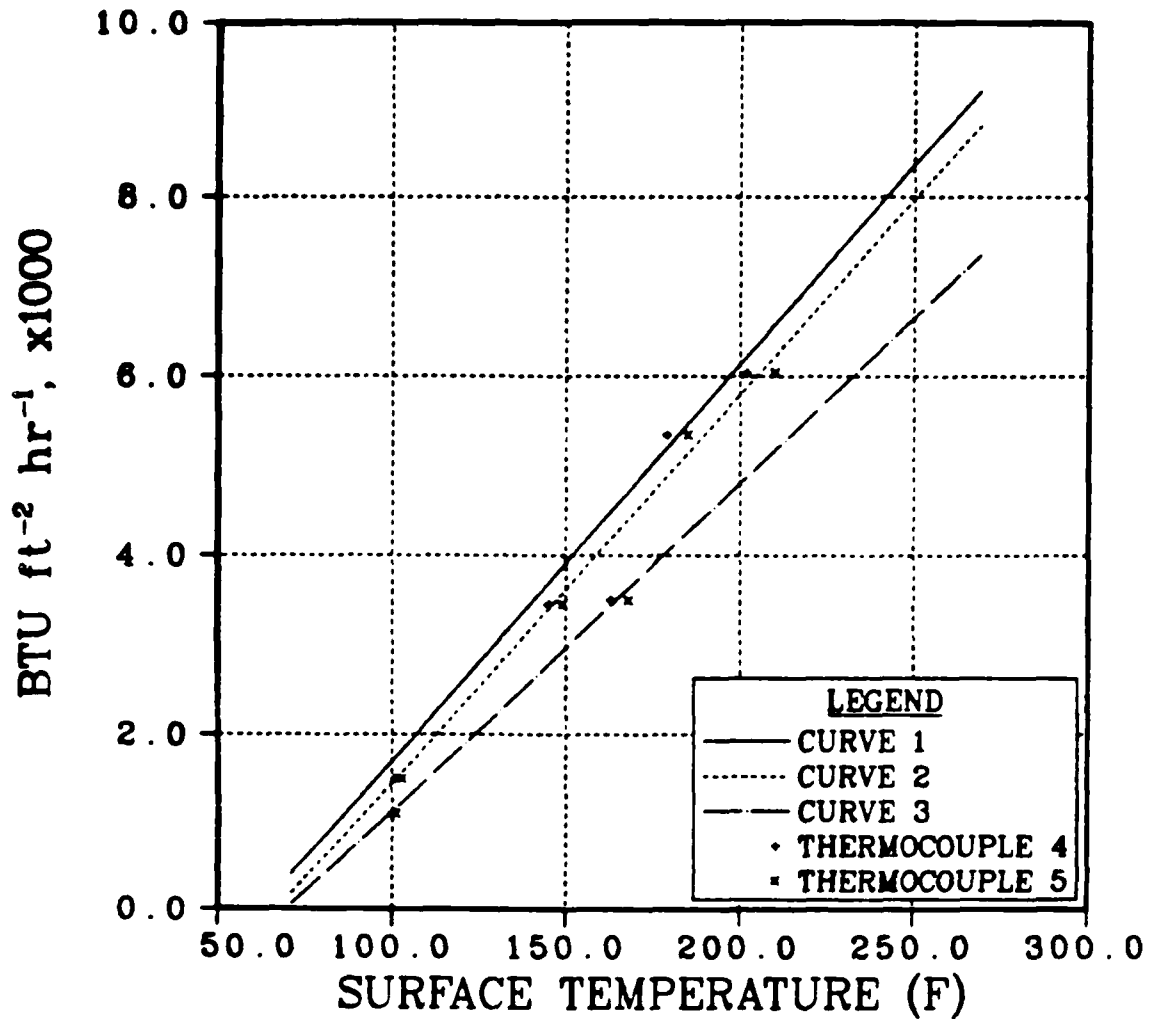
Run No.	Thermocouple of					Heater Power		Air Pressure		Feet per Second	Date	Room Temperature	
	#1	#2	#3	#4	#5	Volts x Amps	Watts	Static lb ft <sup>-2</sup>	Pitot lb ft <sup>-2</sup>				
1	100° F	104	100	92	91	11.25	1.015	11.42	1,441	2,075	842	5/16/79	70° F
2	90	93	90	91	91	11.25	1.015	11.42	1,441	2,075	842	5/16/79	70° F
3	121	129	126	126	127	17.07	1.50	25.6	1,441	2,075	842	5/16/79	70° F
4	180	184	184	184	178	23.4	1.970	46.1	1,441	2,075	842	5/16/79	70° F
5*	178	186	185	185	179	23.4	1.970	46.1	1,441	2,075	842	5/16/79	70° F
6	254	267	275	274	263	31.4	2.49	78.2	1,441	2,075	842	5/16/79	70° F
7	255	272	279	276	266	31.4	2.149	78.2	1,441	2,075	842	5/16/79	70° F
8	111	115	114	114	113	14.18	1.260	17.87	1,441	2,075	842	5/17/79	75° F
9	146	156	157	155	152	19.64	1.695	33.3	1,441	2,075	842	5/17/79	75° F
10	212	227	229	226	219	26.99	2.21	59.6	1,441	2,075	842	5/17/79	75° F
11	100	103	105	103	101.5	12.02	1.08	12.98	1,688	2,103	646	5/17/79	75° F
12	145	150	150	144	145	18.5	1.62	29.97	1,688	2,103	646	5/17/79	75° F
13	201	210	213	210	202	25.1	2.07	51.96	1,688	2,103	646	5/17/79	75° F
14	165	164	169	168	163	18.73	1.61	30.1	1,938	2,108	391	5/17/79	75° F
15	101	100	104	101	100	10.07	.90	9.63	1,938	2,108	391	5/17/79	75° F

\* Shutter forward.



$H = M = 44.0 \text{ BTU ft}^{-2} \text{ hr}^{-1} \text{ F}^{-1}$   
 STATIC PRESSURE =  $1441 \text{ lb ft}^{-2}$   
 PITOT PRESSURE =  $2075 \text{ lb ft}^{-2}$

Fig. A-3 Convective cooling as a function of surface temperature, 70°F and 75°F static temperatures.



$$H = M$$

CURVE 1  $M = 44.0 \text{ BTU ft}^{-2} \text{ hr}^{-1} \text{ F}^{-1}$   
 STATIC PRESSURE =  $1441 \text{ lb ft}^{-2}$   
 PITOT PRESSURE =  $2075 \text{ lb ft}^{-2}$

CURVE 2  $M = 43.5 \text{ BTU ft}^{-2} \text{ hr}^{-1} \text{ F}^{-1}$   
 STATIC PRESSURE =  $1688 \text{ lb ft}^{-2}$   
 PITOT PRESSURE =  $2103 \text{ lb ft}^{-2}$

CURVE 3  $M = 36.75 \text{ BTU ft}^{-2} \text{ hr}^{-1} \text{ F}^{-1}$   
 STATIC PRESSURE =  $1938 \text{ lb ft}^{-2}$   
 PITOT PRESSURE =  $2108 \text{ lb ft}^{-2}$

Fig. A-4 Convective cooling as a function of air speed and surface temperature.

REFERENCES FOR APPENDIX A

1. "Thermal Conductivity of Materials by Mass of a Guarded Hot Plate," American Society for Testing Materials, ASTM-C-177-71.
2. Servias, R. A., Wilt, B. H., and Olson, N. J., "Tri-Service Thermal Radiation Test Facility: Test Procedures Handbook," University of Dayton Research Institute, Dayton, Ohio, UDRI-TR-77-28 (May 1977).
3. Fazekas, F. S. (Captain USAF), "An Analysis of the Tri-Service Thermal Radiation Test Facility," Air Force Institute of Technology Master's Thesis, Wright-Patterson AFB, Ohio, AFIT-GAE-AA-77D-4 (Date).

APPENDIX B  
FRONT SURFACE TEMPERATURE MEASUREMENT FOR  
ABLATING MATERIALS BY SURFACE PYROMETRY

B.1.0 INTRODUCTION

B.1.1 Background

External protection materials (EPM) on the exterior surfaces of long range missiles ablate when exposed to the combined effects of aerodynamic and nuclear thermal radiation heating. It is necessary to consider the total thermal energy from those sources that contribute to heating of the missile's internal structure. The effects of the thermal energy absorbed by the EPM and transmitted to the motor case are predicted by thermodynamic analyses based on materials data from laboratory testing. Applicable laboratory derived data include specific heat versus temperature, thermal conductivity versus temperature, and surface absorptance and emittance. The test of the resultant thermodynamical model is another type of laboratory test.

The Tri-Service Thermal Radiation Test Facility at Wright-Patterson AFB is used for thermal response testing. In that facility, an appropriately instrumented specimen representative of the missile structure and EPM is mounted in a wind tunnel and exposed to a carefully controlled thermal flux. The resultant thermal response of the specimen ideally will match those predicted by the thermodynamical model. Quite often, the error lies not just in the analytical model, but in the laboratory data used to support the analyses.

Typical test methods for determining specific heats, thermal conductivities, and absorptance of materials are applicable only at temperatures lower than the temperatures at which the materials begin to incur permanent change or degradation. Above these temperatures, many materials properties, including the thermal properties, are both time and temperature dependent. Conventional testing methods are useless at these high temperature conditions and extrapolated lower temperature data is frequently used to support the analytical program. A reiterative process



based on the thermal flash test results can be applied to correct the extrapolated data. Essential to this process is accurate front surface temperature data.

#### B.1.2 Purpose

The purpose of this appendix is to document test procedures developed to determine front-surface temperatures of ablating materials at the Tri-Service Thermal Radiation Facility and some examples of data resultant from those test procedures.

#### B.2.0 DISCUSSION

##### B.2.1 Approach

Two independent methods were chosen for the attempt to measure the temperature of an ablating surface. Method one employed .001 in. (.0025 mm) chromel-alumel thermocouples, the second method employed infrared pyrometry.

##### B.2.2 Method One--Surface Temperature by Means of Thermocouples

Thermocouples applied directly to a surface which is to be irradiated by a high energy source cannot be expected to result in meaningful surface temperature data for the following reasons:

- The thermocouple junction will absorb energy directly from the source at a rate different from the parent surface.
- The thermocouple junction will very quickly debond from the surface at a temperature lower than the ablation temperature.
- When used in conjunction with a windstream, the junction will significantly perturb the windstream and will be directly heated or cooled by it.
- Adhesives must be used to mount the thermocouple which in themselves represent a significant thermal mass.

The method employed in this case utilizes subsurface thermocouples. As a specimen is irradiated, these thermocouples will indicate a temperature lower than the surface. As the surface recedes, the thermocouple comes closer to the surface; the thermocouple will approach the temperature of the surface. At the instant the junction is exposed either one of two events can be expected to occur:

- The thermal radiation incident on the junction will sharply increase the indicated temperature.
- The convective cooling associated with the wind tunnel will overpower the radiative effects and sharply reduce the junction temperature.

In either event the indicated temperature will be in error. The junction will indicate approximately the surface temperature for about a tenth of a second.

The thermocouples selected for these tests were .001 in. (.0025 mm) diameter chromel-alumel. Two specimens of ablative materials were tested by this method. They were VAMAC 151A and VAMAC 151B. These materials were supplied by Martin Marietta Aerospace Corporation. The specimens were prepared by slitting each test material nearly through the thickness with a surgical knife. The slits were approximately one inch long. The VAMAC slabs were then bent slightly to force the slits open. Thermocouple junctions were then laid in the slits, and the slits were allowed to close. These slabs were then bonded to bakelite backing plates with a silicone adhesive.

Figure B-1 represents the resultant specimen configuration. These specimens were also used for the front surface pyrometry tests. During the testing, the results of each test influenced the interpretation of the other. As a result, both test results will be discussed concurrently in Section 3.0.

#### B.2.3 Method Two--Infrared Pyrometry

This method is designed to take advantage of the spectral characteristics of the Tri-Service Thermal Radiation Test Facility's thermal source.

This facility utilizes as a source quartz-tungsten lamps behind a quartz window. The tungsten filaments are operated at a nominal color temperature of 3000°K. Figure B-2 shows the spectral emission characteristics of tungsten at 3000°K and the transmission characteristics of quartz. Quartz is an effective filter from 5.3 microns to beyond 25 microns. The thermal source is therefore deficient in energy in this wave length region. However, any specimen heated by this source would emit energy strongly in this region. All that is required for effective pyrometry is to select a detector that is sensitive only to wave lengths in excess of 5.3 microns. In this case, a thermopile detector made by Dextor Corp. was selected. The thermopile itself has a very flat, broad-band spectral response. This particular detector was fitted with a 6.8 micron cut-on filter. Figure B-3 illustrates the transmission characteristics of this filter. This detector was mounted in an air-cooled housing. A light pipe constructed from a curved copper tube was designed to direct infrared energy from the surface of a specimen mounted in the Tri-Service Thermal Radiation Facility to an area where the detector assembly could be mounted. Figure B-4 illustrates the resultant arrangement.

There are several important factors to consider when infrared pyrometry is to be used in such applications. Of primary importance is the selection of a valid calibration procedure. In this series of tests, a blackened .060 in. (1.52 mm) thick copper plate was selected as a medium for calibration. A .005 in. (.127 mm) chromel-alumel thermocouple was welded to the back of the copper plate. This assembly was then loosely mounted in a transite asbestos block, and the combination was mounted in the wind tunnel specimen port. In this position, the copper plate was viewed by the pyrometer. The copper plate was then rapidly heated by energizing the lamp bank. Both the output of the thermocouple on the back of the copper plate and the output of the pyrometer were recorded on a three axis (X-Y-Y') recorder. A total of nine calibration runs were performed. These data resulted in the calibration curve shown in Figure B-5.

Several additional runs were performed with nothing in the specimen port verifying that no extraneous signal was being picked up by the pyrometer. One run each was conducted in which the pyrometer sampled the energy from the lamps reflected from  $\frac{1}{2}$  in. (1.27 cm) thick polished aluminum plate and a

similar blackened aluminum plate. In each case, the reflected energy was insignificant.

One primary assumption is necessary to this calibration procedure. The absorptance of the test specimen during ablation or any point of interest is approximately equal to the absorptance of the copper plate at the same temperature. Figure B-6 is a comparison of the room temperature absorptances of the copper plate and the post-test absorptances of the two VAMAC materials in the wave length range that the pyrometer operates. They are obviously quite similar. The assumption then becomes a matter of the equivalence of their relative high temperatures absorptances. Since the copper plate was blackened with carbon, and carbon is the predominant material used as a filler in the test specimens and is evident on the ablating surface, this assumption is considered valid.

Section B.6.0 is an error analysis that indicates a 5% error in absorptance could be expected to produce an error of less than 35°K at an actual temperature of 1000°K. This is considered within the limits of the desired accuracy.

### B.3.0 RESULTS

All specimens were subjected to  $30 \text{ cal/cm}^2/\text{sec}$  for three seconds. Figures B-7 through B-19 represent the data obtained from the two different test methods.

The first specimen tested was VAMAC 25 supplied by McDonnell-Douglas, Huntington Beach, California. There were no thermocouples in the volume of this specimen. There was one back-surface thermocouple. Based on previous computer predictions, the pyrometer was set to 1000°F (810 K) full scale. As the specimen was flashed, the pyrometer went off scale. Figure B-7 represents the results of retesting this first specimen. The specimen had a distinct char layer prior to the test. Apparent is an initial peak temperature of 2904°F (1868 K) and a stabilized temperature of 1400°F (1033 K).

Figure B-8 represents a test of VAMAC 151B. In this test, an initial peak temperature is again evidenced; however, it is greatly reduced. The

peak temperature is 1346°F (1063 K), with a final temperature of 1204°F (424 K).

Figure B-9 represents a second sample test of VAMAC 151B. The results did not show an initial peak as was seen in Figure B-8. The temperature rose to an almost constant 1120°F (877 K).

Figure B-10 is the result of a  $30 \text{ cal/cm}^2/\text{sec}$ , three second test of VAMAC 151A. The initial temperature rise was to 1208°F (926 K), with a steady-state temperature of approximately 1140°F (889 K).

Figure B-11 is the result of the second VAMAC 151A sample tested. This specimen exhibited an initial temperature rise of 1137°F (887 K). It apparently would have stabilized at 910°F (761 K).

Figure B-12 shows the test results of a Royacril specimen. The surface temperature rapidly rose to 1160°F (900 K) and remained nearly constant for the duration of the pulse.

Figure B-13 is the result of the first flash of a specimen of VAMAC 151A with the imbedded subsurface thermocouple. The initial temperature rise was 1119°F (277 K), with stabilization at 900°F (755 K). The thermocouple registered 422°F (490 K) maximum. Since its temperature was still rising after the shutter was closed, it was not yet exposed at the surface.

Figure B-14 is a retest of the sample used in Figure B-13. The initial temperature was 1114°F (874 K), with stabilization at 924°F (769 K). The thermocouple rose to 736°F (664 K). A close examination of the raw data shows that the thermocouple indicated temperature was still rising after the shutter closed, indicating that it had not reached the surface by surface recession.

Figure B-15 is a second retest of the Figure B-13 specimen. The pyrometer indicated 1317°F (487 K) at peak, and 1080°F (855 K) at stabilization. The thermocouple rose to 1495°F (1086 K) and abruptly dropped. The drop was prior to shutter closure. At this point, the pyrometer indicated 1019°F (821 K). The recorded temperature decay indicates, however, that the

thermocouple is still just barely subsurface because the pyrometer shows a more rapid decay than the thermocouple.

Figure B-16 is a third retest of the previously tested specimen. The pyrometer registered a similar peak temperature of 1175°F (908 K) with a stabilized temperature of 1050°F (839 K). The thermocouple rose to 1448°F (1060 K) and dropped to a temperature less than that indicated by the pyrometer. It had undoubtedly been exposed to the airstream. That fact is confirmed by the decay portion of these curves. After this test, the thermocouple junction was (just barely) visibly exposed.

Figure B-17 is the result of the first of a series of tests involving a VAMAC 151B specimen with an imbedded subsurface thermocouple. The pyrometer indicated a flat response at 990°F (805 K). The thermocouple rose to 298°F (421 K). The surface was hotter than the subsurface thermocouple.

Figure B-18 illustrates a retest of the specimen of Figure B-17. The peak shown for the pyrometer is at 1265°F (958 K), with an equilibrium temperature of about 1085°F (858 K). The subsurface thermocouple indicated a maximum temperature of 513°F (540 K), which was cooler than the surface.

Figure B-19 shows the results of a second retest of the VAMAC 151B specimen with the subsurface thermocouple. The pyrometer shows a peak temperature of 1265°F (958 K) with a steady-state 1080°F (855 K) plateau. The subsurface thermocouple peaked at 1364°F (1013 K). It dropped in temperature before the shutter was closed. Post-test analysis indicated an exposed thermocouple.

The average peak and equilibration temperatures of the three materials tested as measured by surface pyrometry are summarized in Table B-1.

The VAMAC 25 specimen had been tested twice, but data was available only for the second test. The two specimens with subsurface thermocouples indicate that the surface temperature of ablating VAMAC 151A is 1514°F (1096 K) and VAMAC 151B is 1364°F (1013 K). These are single point data.

TABLE B-1  
SUMMARY OF SURFACE PYROMETRY EXPERIMENTS

	<u>Avg. Peak, °F</u>	<u>Equilibration, °F</u>
VAMAC 151A	1161 (900 K)	1030 (827 K)
VAMAC 151B	1206 (925 K)	1098 (865 K)
VAMAC 25	1904 (1313 K)	1380 (1022 K)
Royacril	1166 (903 K)	1166 (903 K)

Two different models can be constructed to explain the difference between the thermocouple data and the pyrometer data. The first is that the thermocouple data is more accurate. When the surface begins to ablate, smoke is produced that obscures the view of the pyrometer from the ablating surface. The second, somewhat more complex theory, is that the pyrometer is correct. Therefore, the surface is cooler in some cases than the subsurface thermocouple. Either local enthalpy is driving the thermocouple hotter, or the surface char is selectively transparent (transparent to the lamp bank spectrum and not the pyrometer spectrum) and the surface of the char is being cooled by convective cooling and/or transpiration cooling. In either case, the temperature of the ablating surface is certainly greater than 1000°F (811 K) throughout the ablation time.

#### B.4.0 RECOMMENDATIONS

Additional work is required to perfect the front surface pyrometry into an accurate useful tool. Studies should be directed to resolve and quantify the smoke occlusion hypothesis, and to determine if the data scatter results from the variability in the pyrometer, or if the data scatter results from changes from specimen to specimen in the ablation processes.

#### B.5.0 ERROR ANALYSIS

These analyses are based on an uncertainty in surface emissivity of 0.05 (as compared to the calibration standard).

## TOTAL ENERGY

The Stefan-Boltzman law states

$$W = \epsilon \sigma T^4$$

where:

$W$  = total radiant flux emitted per unit area,

$\epsilon$  = emittance,

$\sigma$  = Stefan-Boltzman constant, and

$T$  = absolute temperature of a radiating body in degrees Kelvin.

Take  $\epsilon_1$  to be the actual surface emittance and  $\epsilon_2$  to be the assumed emittance where

$$\epsilon_1 = \epsilon_2 - 0.05$$

$$W_1 = \epsilon_1 \sigma T_1^4 \quad \text{where } T_1 = \text{actual surface temperature}$$

$$W_2 = \epsilon_2 \sigma T_2^4, \quad T_2 \text{ is a computed value based on } W_2 \text{ and an assumed } \epsilon_2$$

$$W_1 = W_2 \quad (\text{a measured quantity})$$

then

$$\epsilon_1 \sigma T_1^4 = \epsilon_2 \sigma T_2^4$$

$$\frac{1}{\epsilon_2} = \frac{T_2^4}{T_1^4}$$

In the experiment conducted,  $T_1 \approx 1000^\circ\text{K}$ .



Therefore

$$T_2^4 = \frac{1}{1.05} \times T_1^4 = 0.952 \times 10^{12}$$

$$T_2 = 988^\circ \text{ K}$$

The error,  $T_1 - T_2$ , is  $12^\circ\text{K}$ .

#### IN-BAND ENERGY FROM PLANCK'S RADIATION LAW

Assume that the detector responds equally to all energy incident between 6.8 microns and 17 microns. Assume that the emitting surface is actually  $1000^\circ\text{K}$ . If  $\epsilon$  were 1.0, the surface would radiate 1.014 watt/sq cm. If, however, the effective  $\epsilon$  in this wave length band were not 1.0 but 0.95, the surface would radiate  $0.95 \times 1.014 = 0.964$  watts/sq cm. This is equivalent to the energy from a  $965^\circ\text{K}$  source with an  $\epsilon$  of 1.0.

The error resulting from an uncertainty of 0.05 in surface emittance between the test specimen and calibration specimen is approximately  $1000^\circ\text{K} - 965^\circ\text{K}$  or  $35^\circ\text{K}$ .

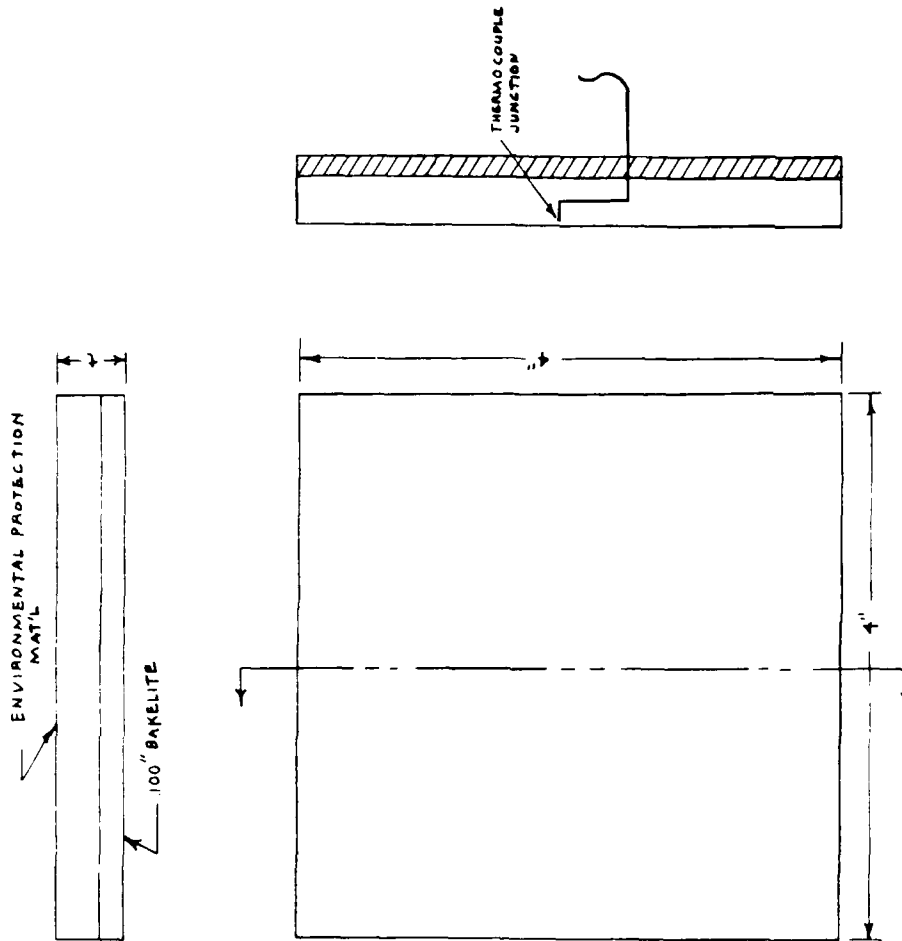


Fig. B-1 Specimen configuration.

Notes: "t" is not to scale, typically .250".  
 EPM is bonded to bakelite with .001" silicone adhesive.  
 1" = 2.54 cm.

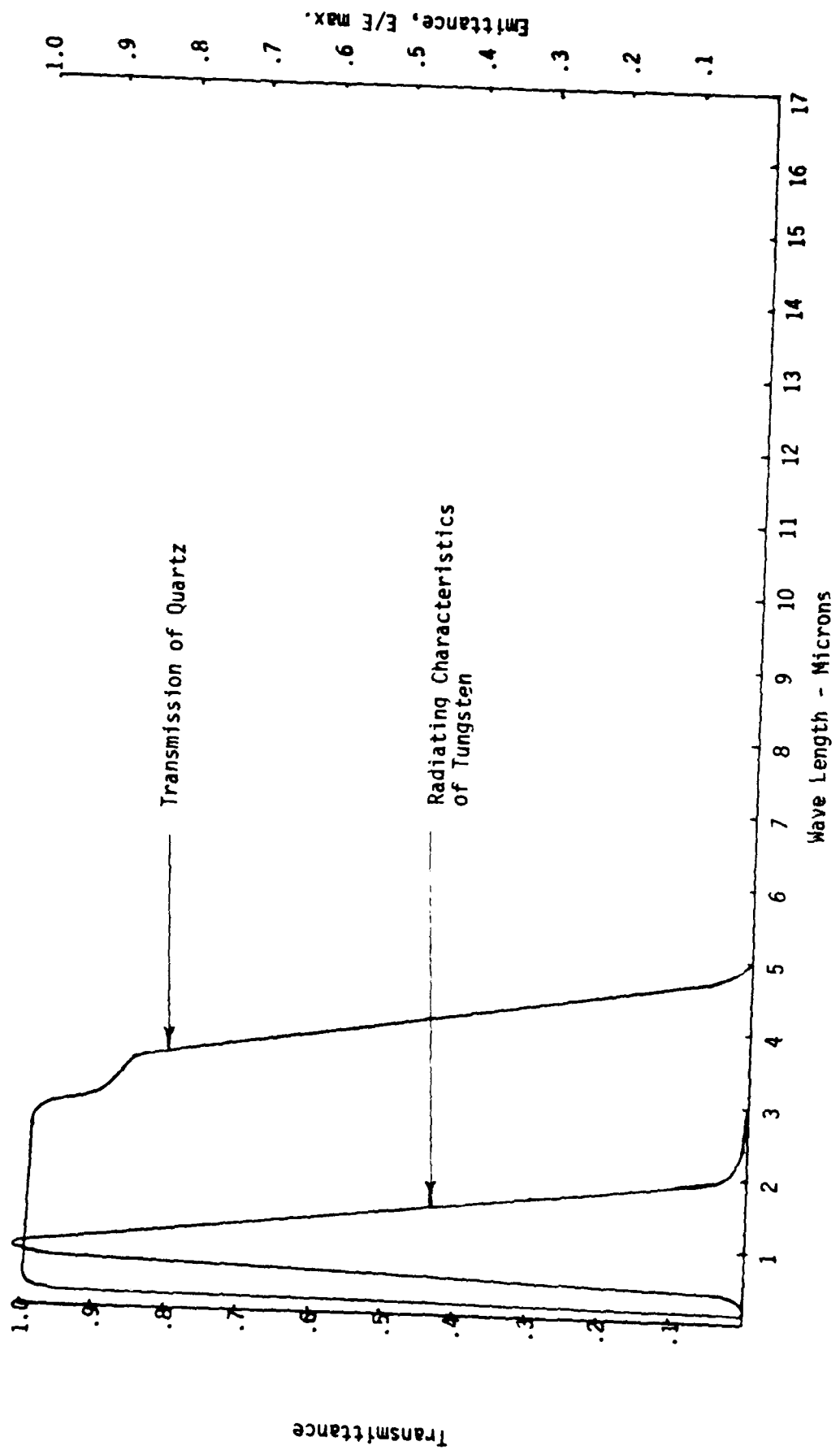


Fig. B-2 Transmittance of quartz and emission of a 3000°K tungsten filament.

Transmittance

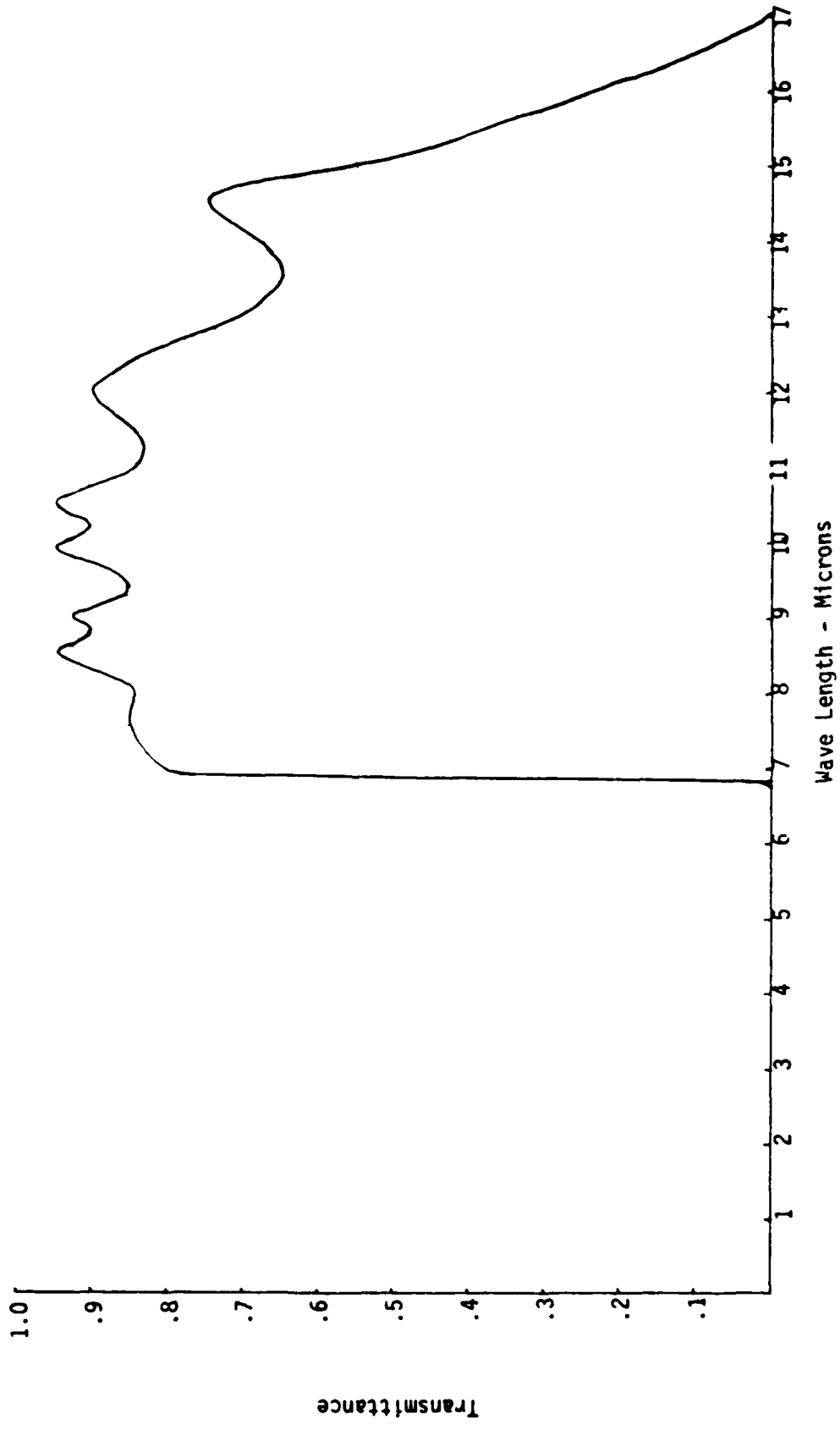


Fig. B-3 6.8 micron cut-on filter transmittance.

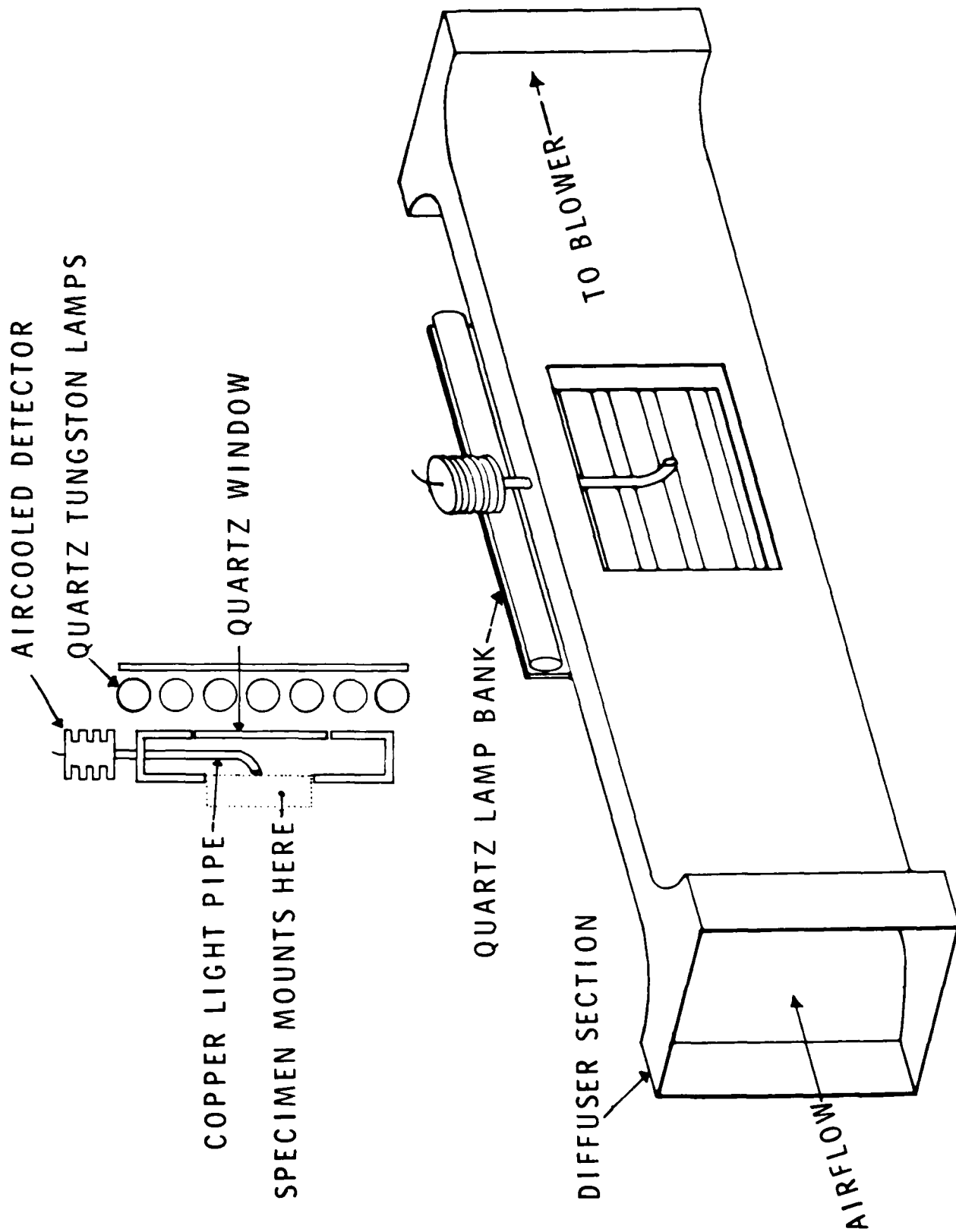


Fig. B-4 Pyrometer positioned in wind tunnel.

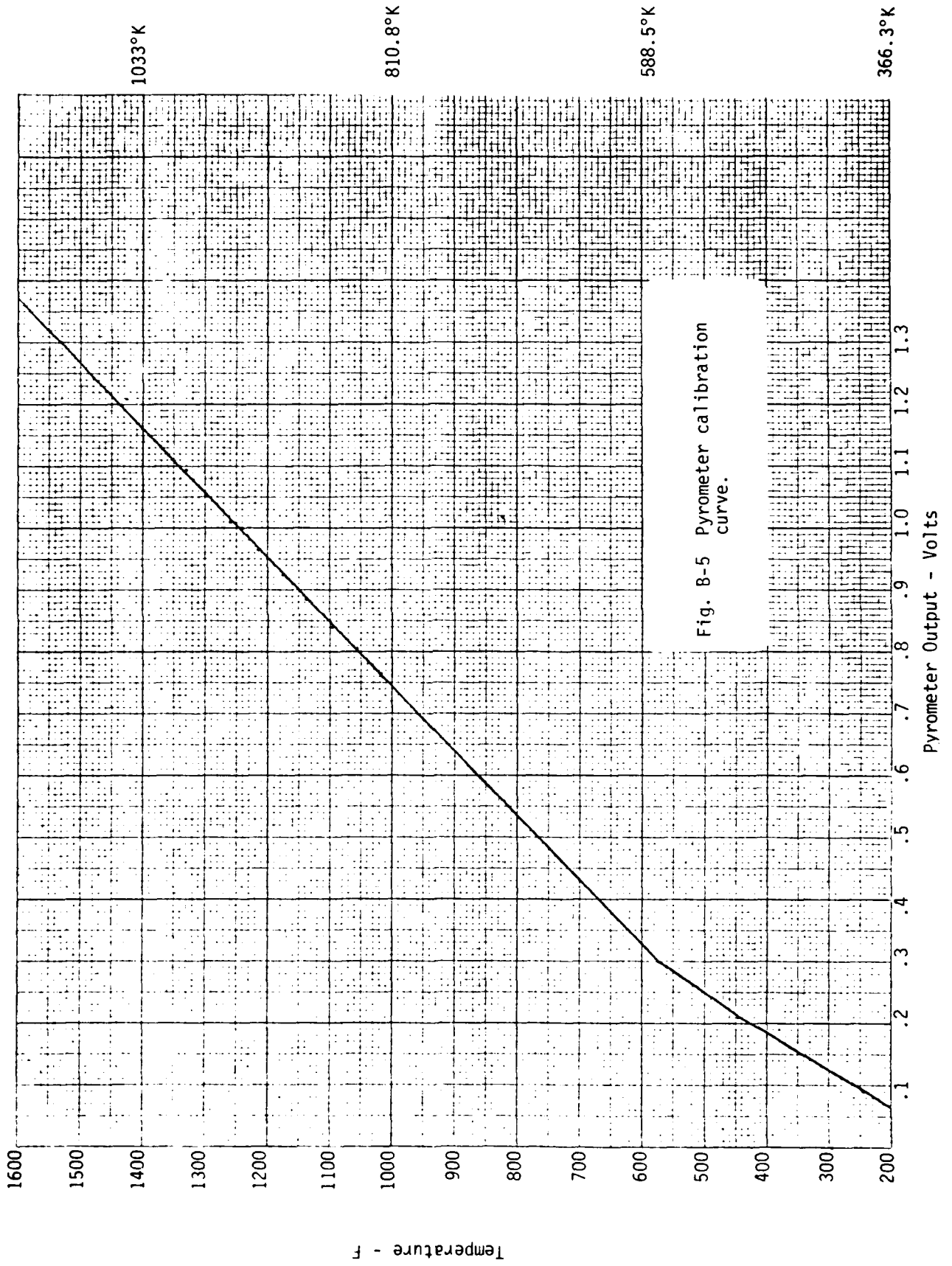


Fig. B-5 Pyrometer calibration curve.

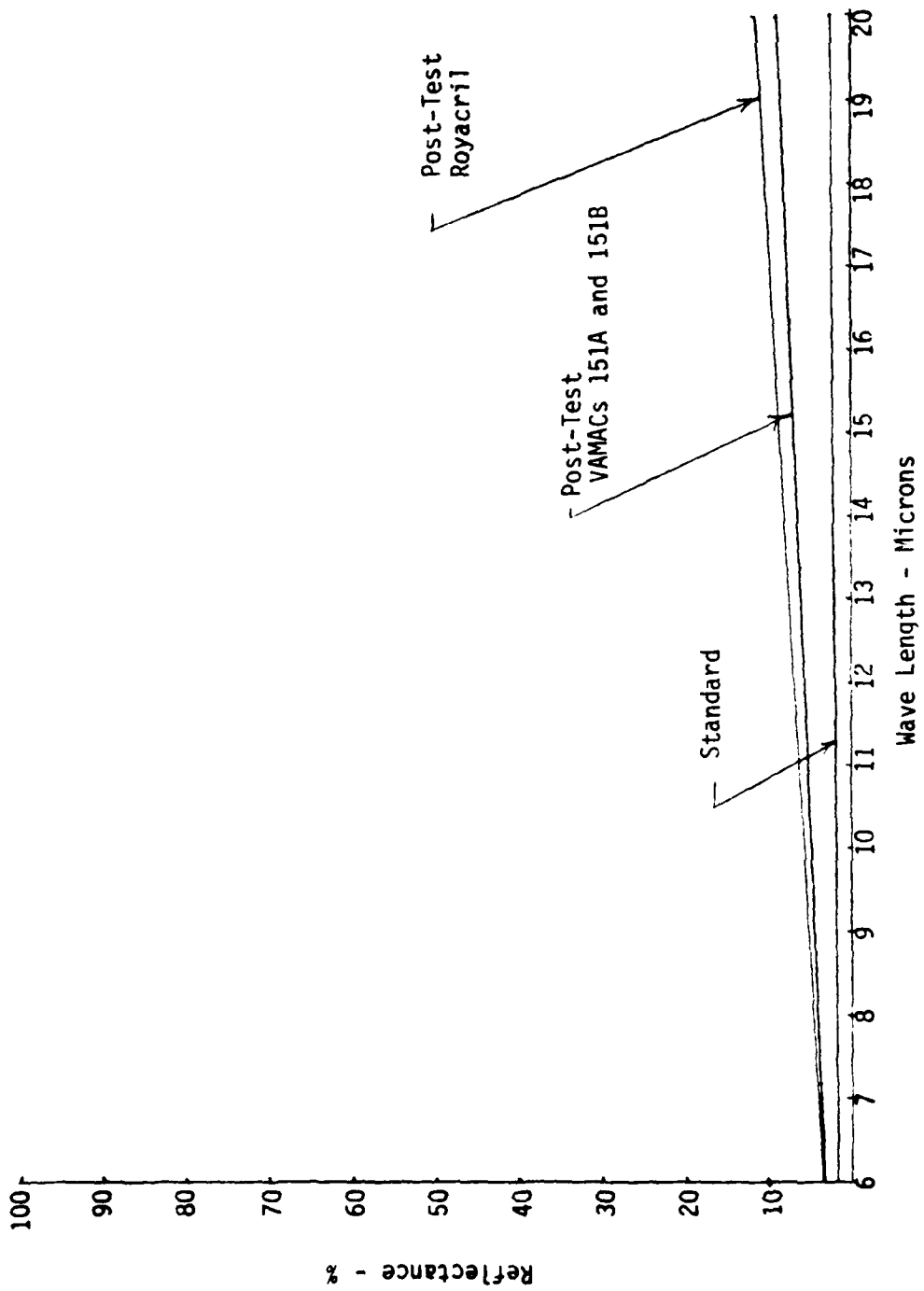
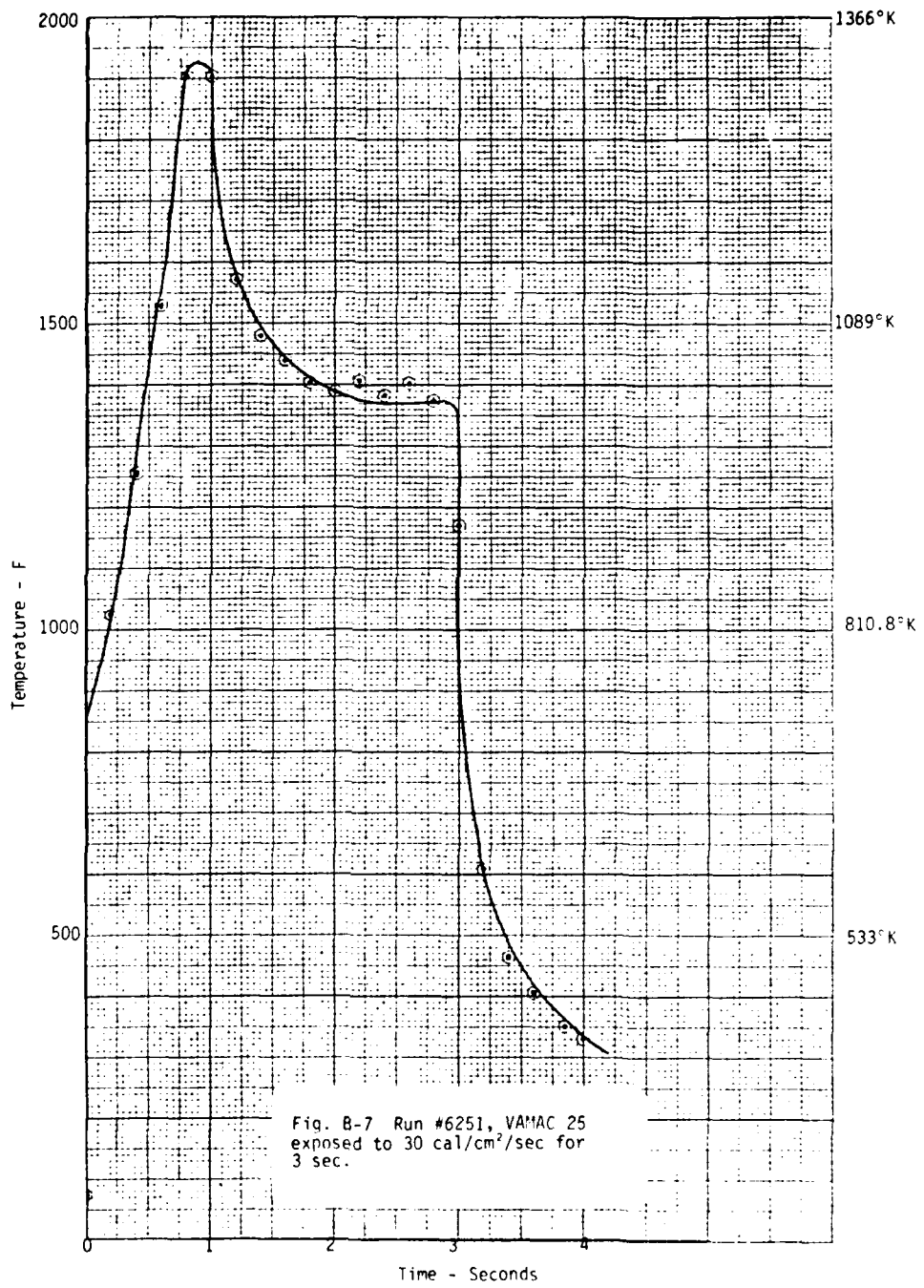
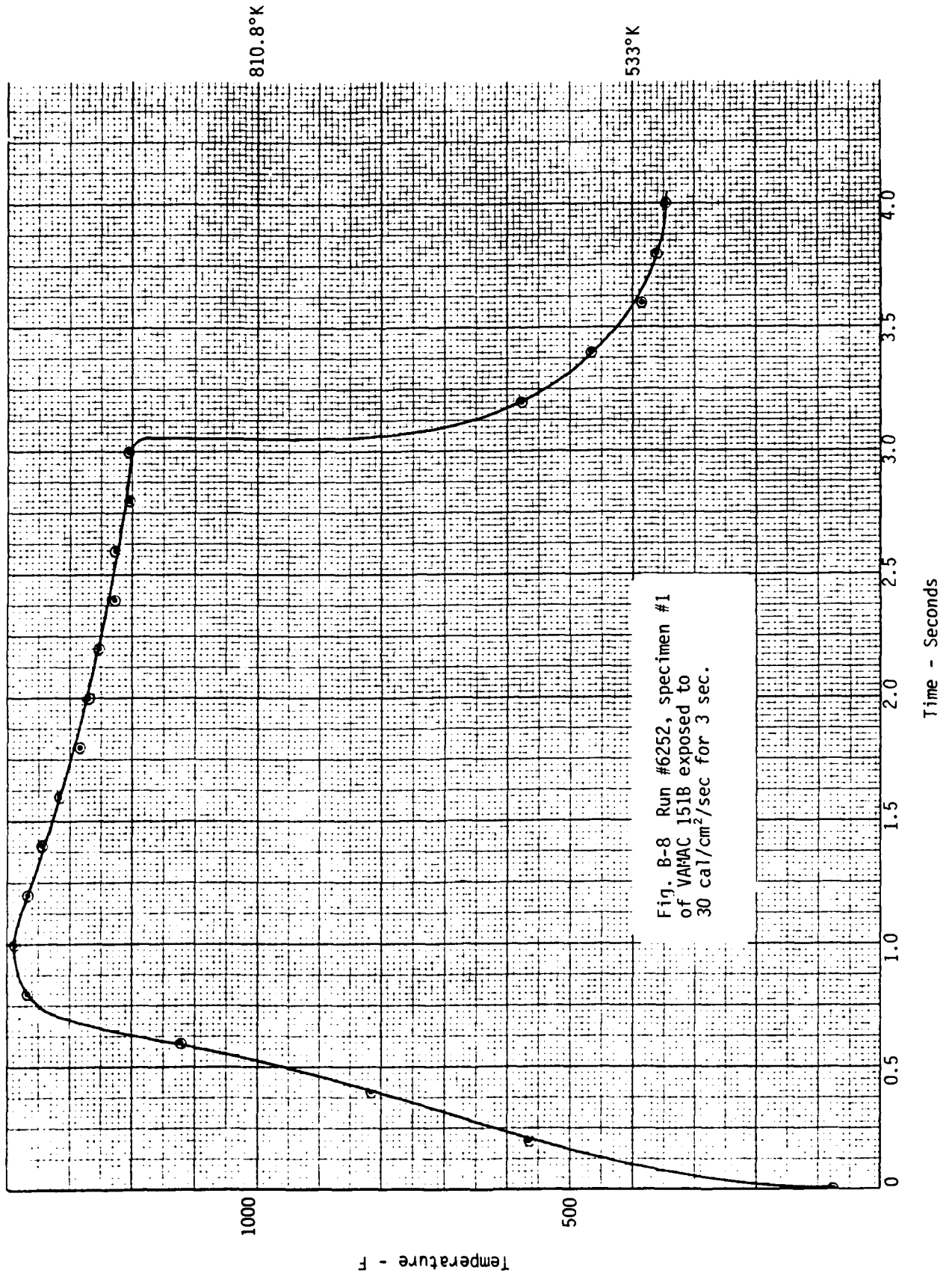


Fig. B-6 Infrared reflectance of test material.







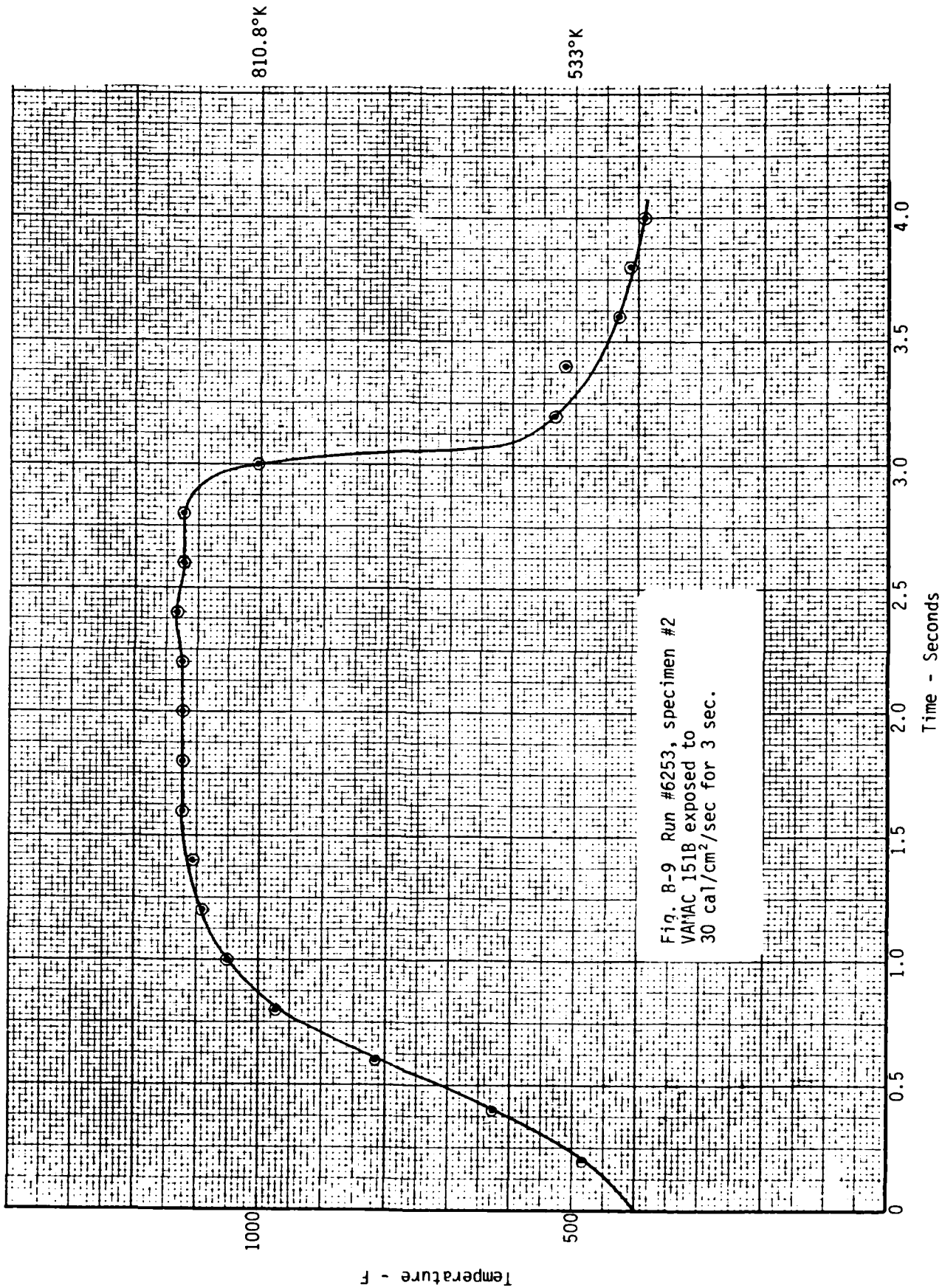


Fig. B-9 Run #6253, specimen #2  
 VAMAC 151B exposed to  
 30 cal/cm<sup>2</sup>/sec for 3 sec.

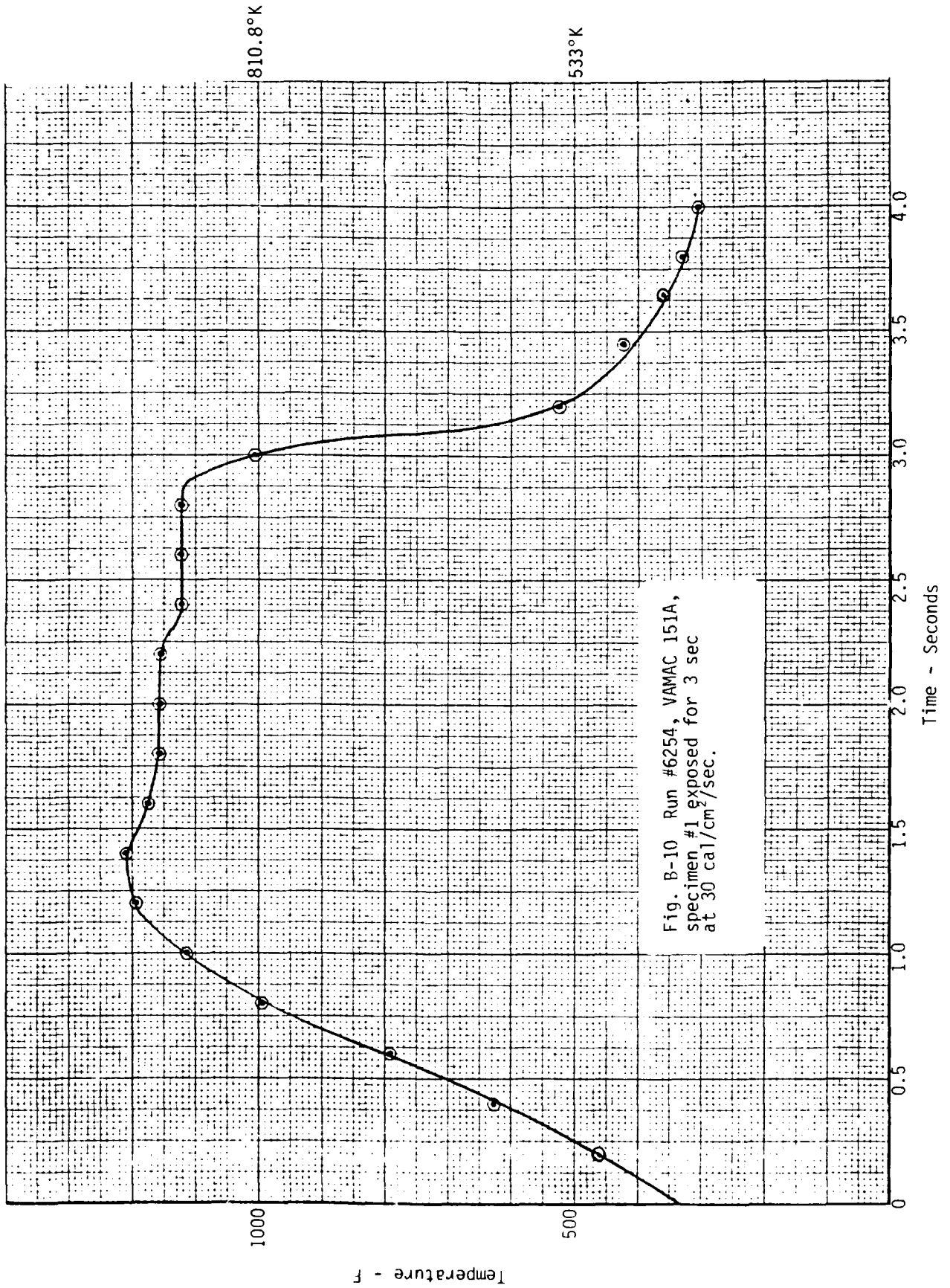


Fig. B-10 Run #6254, VAMAC 151A, specimen #1 exposed for 3 sec at 30 cal/cm<sup>2</sup>/sec.

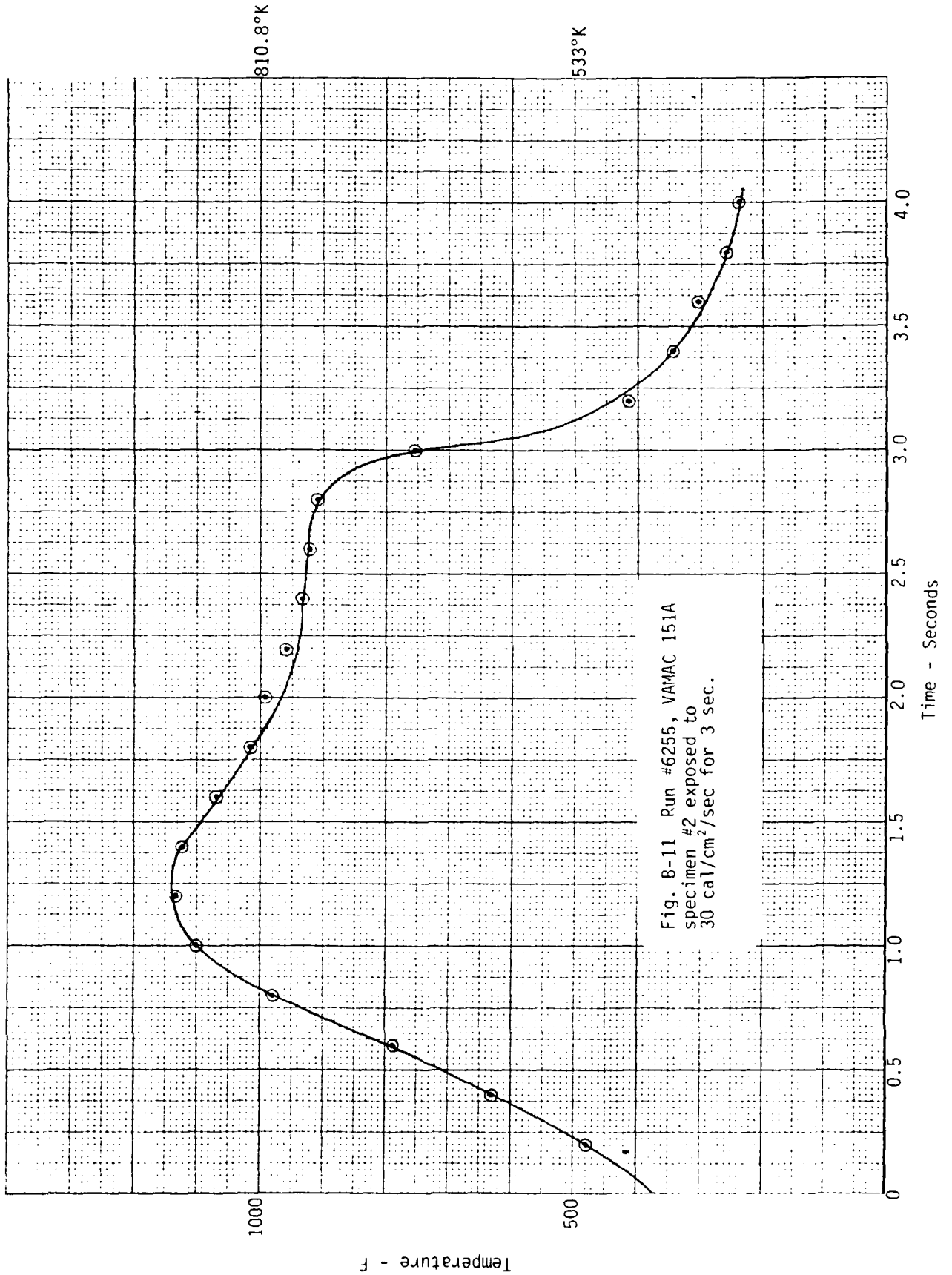


Fig. B-11 Run #6255, VAMAC 151A  
specimen #2 exposed to  
30 cal/cm<sup>2</sup>/sec for 3 sec.

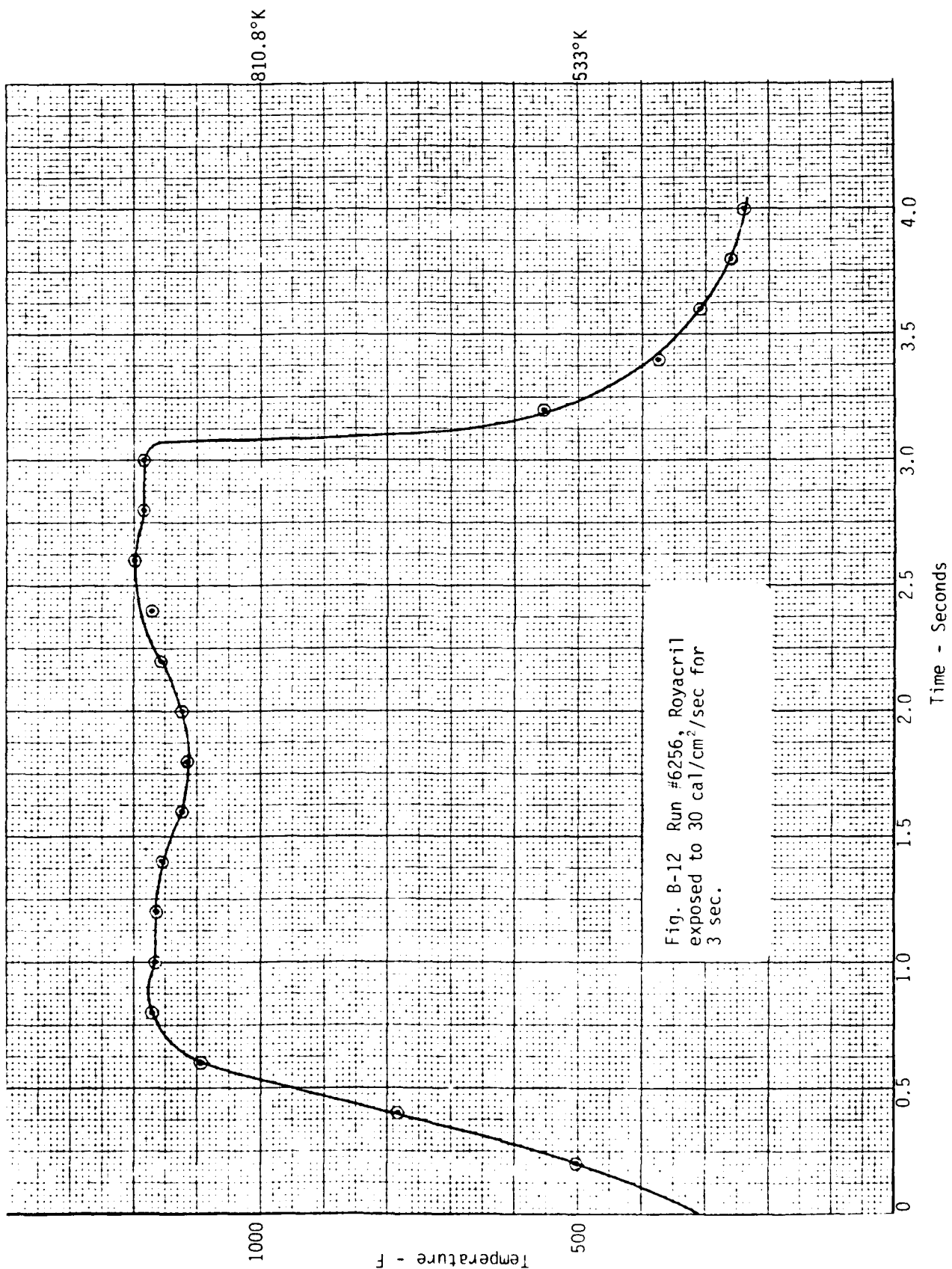


Fig. B-12 Run #6256, Royacril exposed to 30 cal/cm<sup>2</sup>/sec for 3 sec.

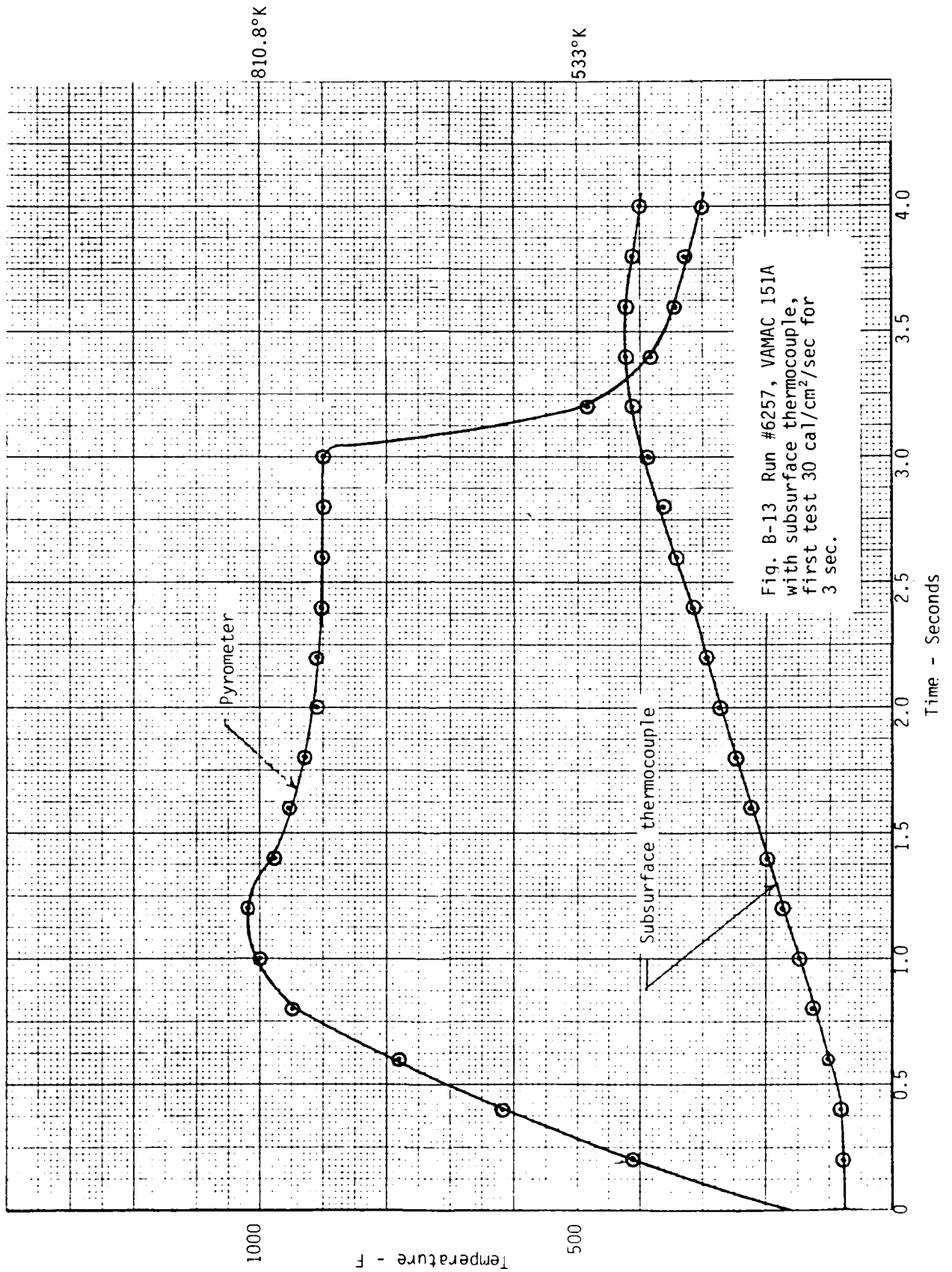


Fig. B-13 Run #6257, VAMAC 151A  
with subsurface thermocouple,  
first test 30 cal/cm<sup>2</sup>/sec for  
3 sec.

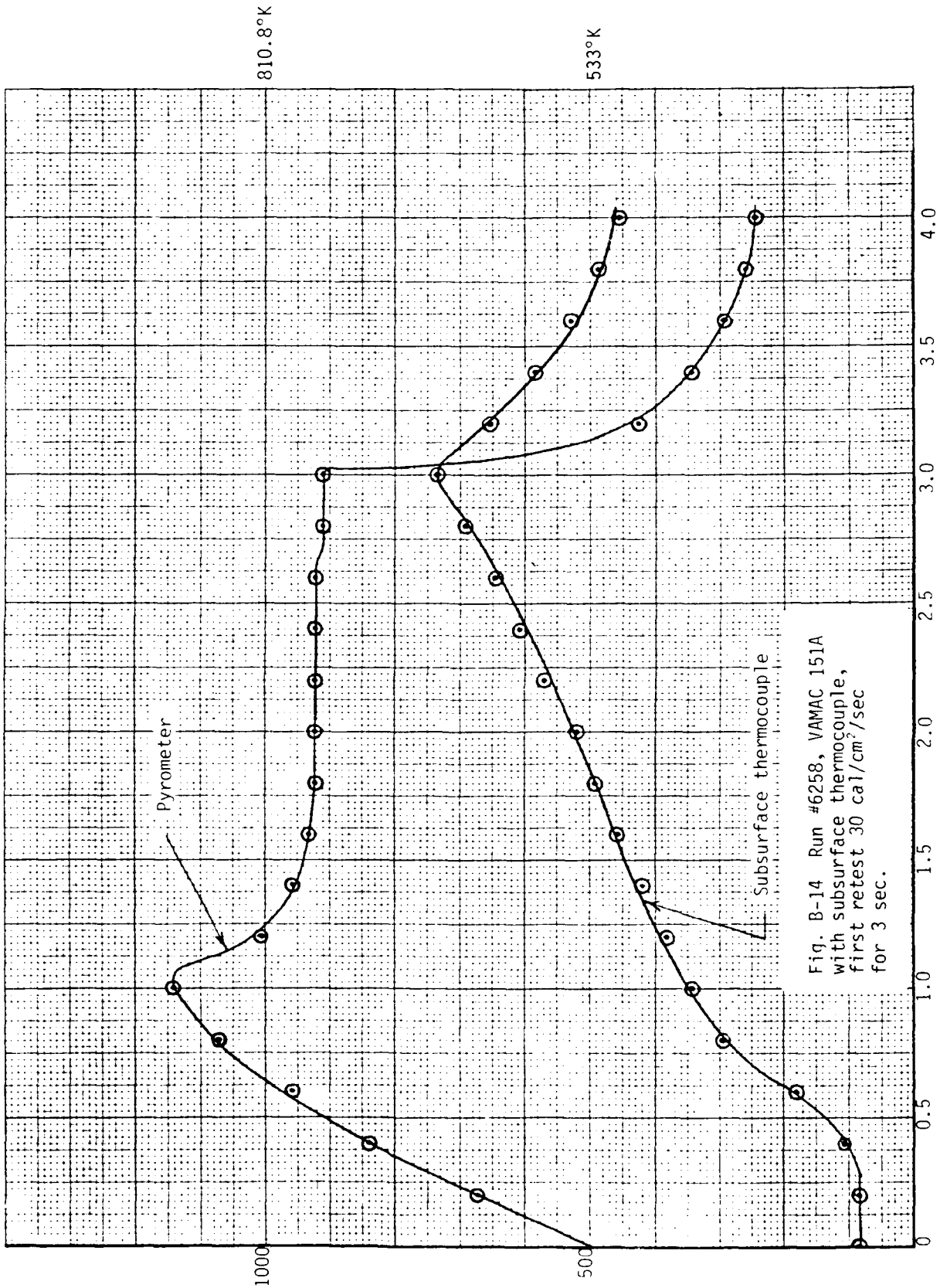


Fig. B-14 Run #6258, VAMAC 151A with subsurface thermocouple, first retest 30 cal/cm<sup>2</sup>/sec for 3 sec.

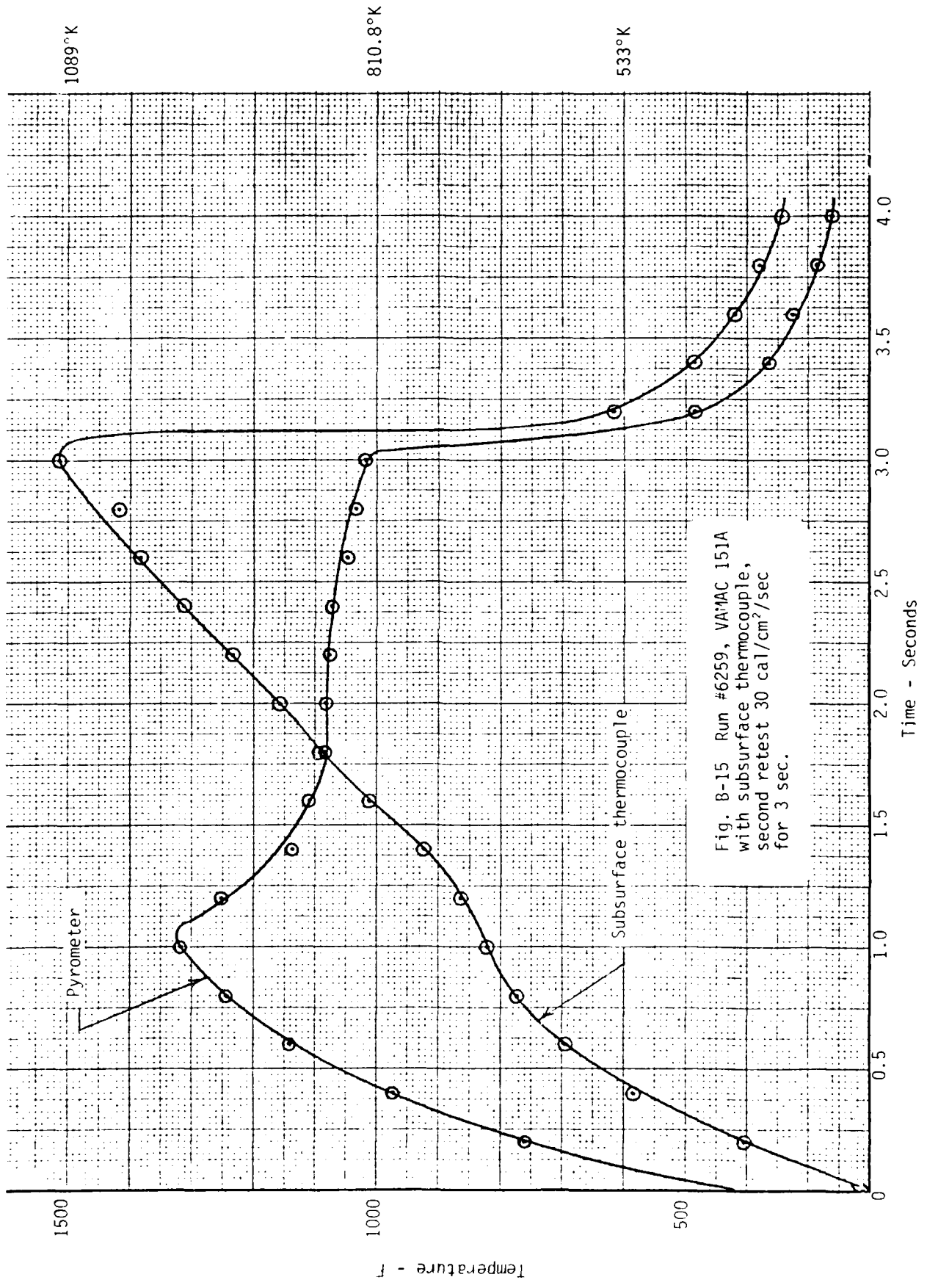


Fig. B-15 Run #6259, VA-MAC 151A  
 with subsurface thermocouple,  
 second retest 30 cal/cm<sup>2</sup>/sec  
 for 3 sec.



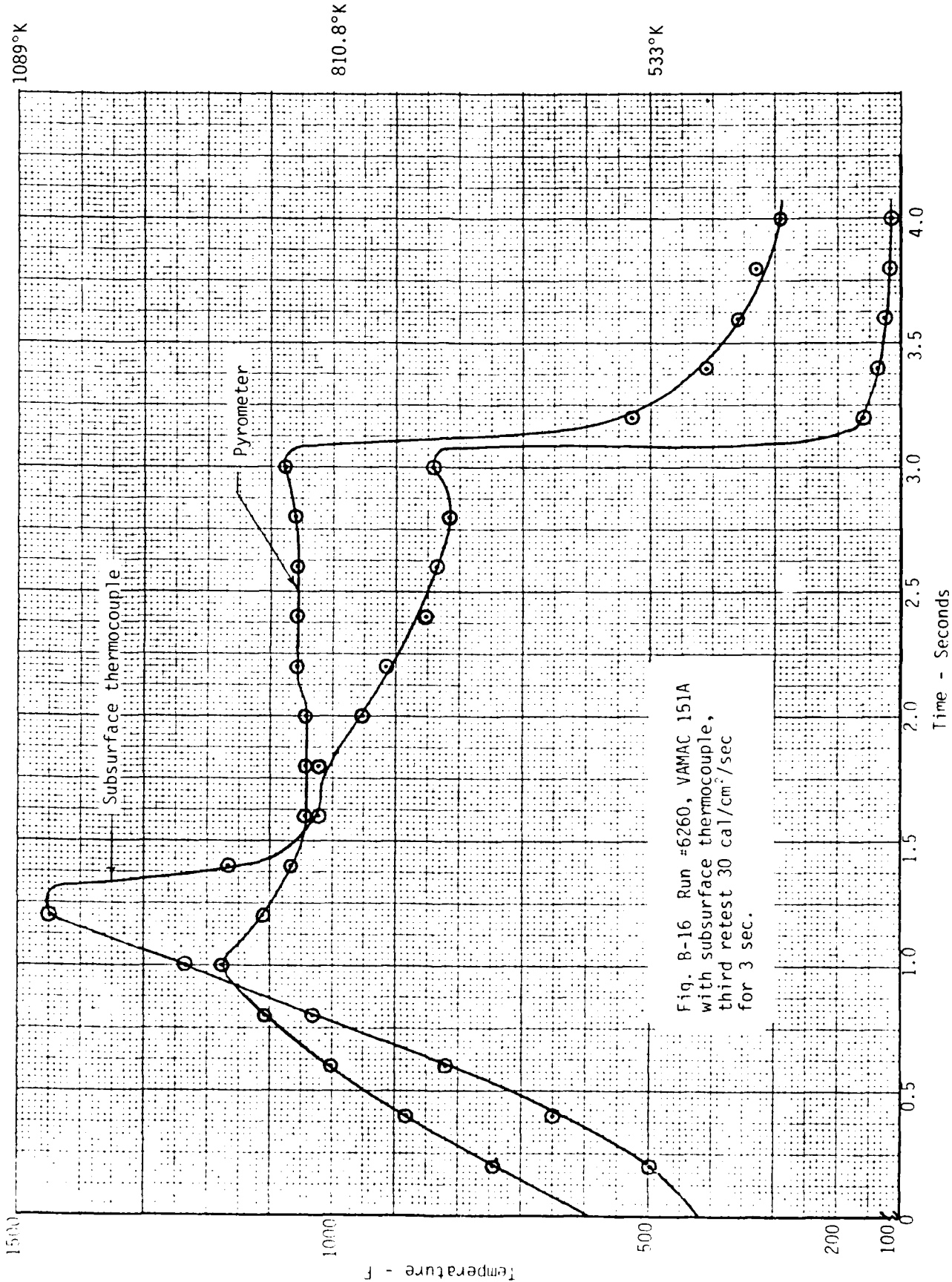


Fig. B-16 Run #6260, VAMAC 151A with subsurface thermocouple, third retest 30 cal/cm<sup>2</sup>/sec for 3 sec.

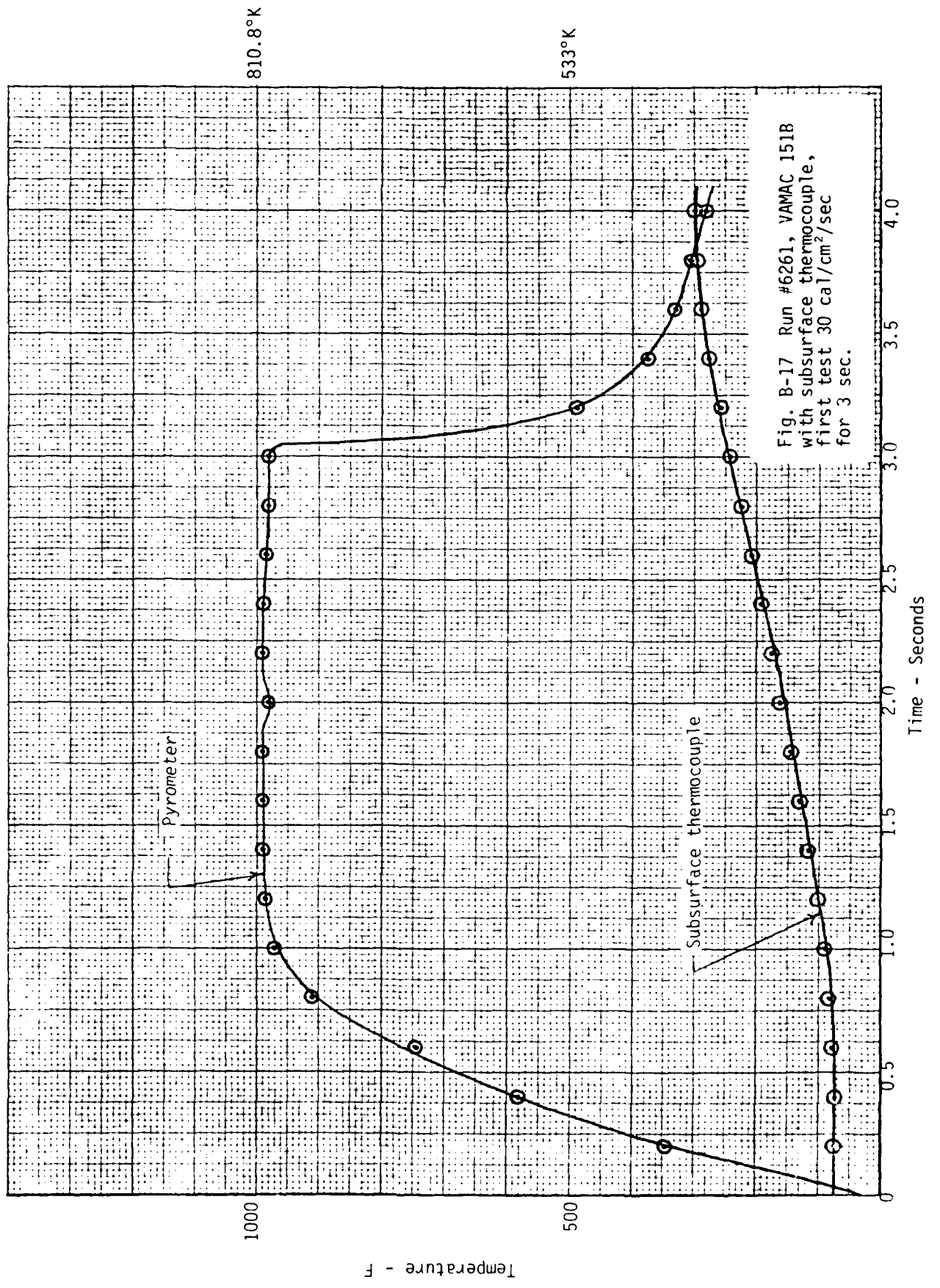


Fig. B-17 Run #6261, VAMAC 151B with subsurface thermocouple, first test 30 cal/cm<sup>2</sup>/sec for 3 sec.

Temperature - F

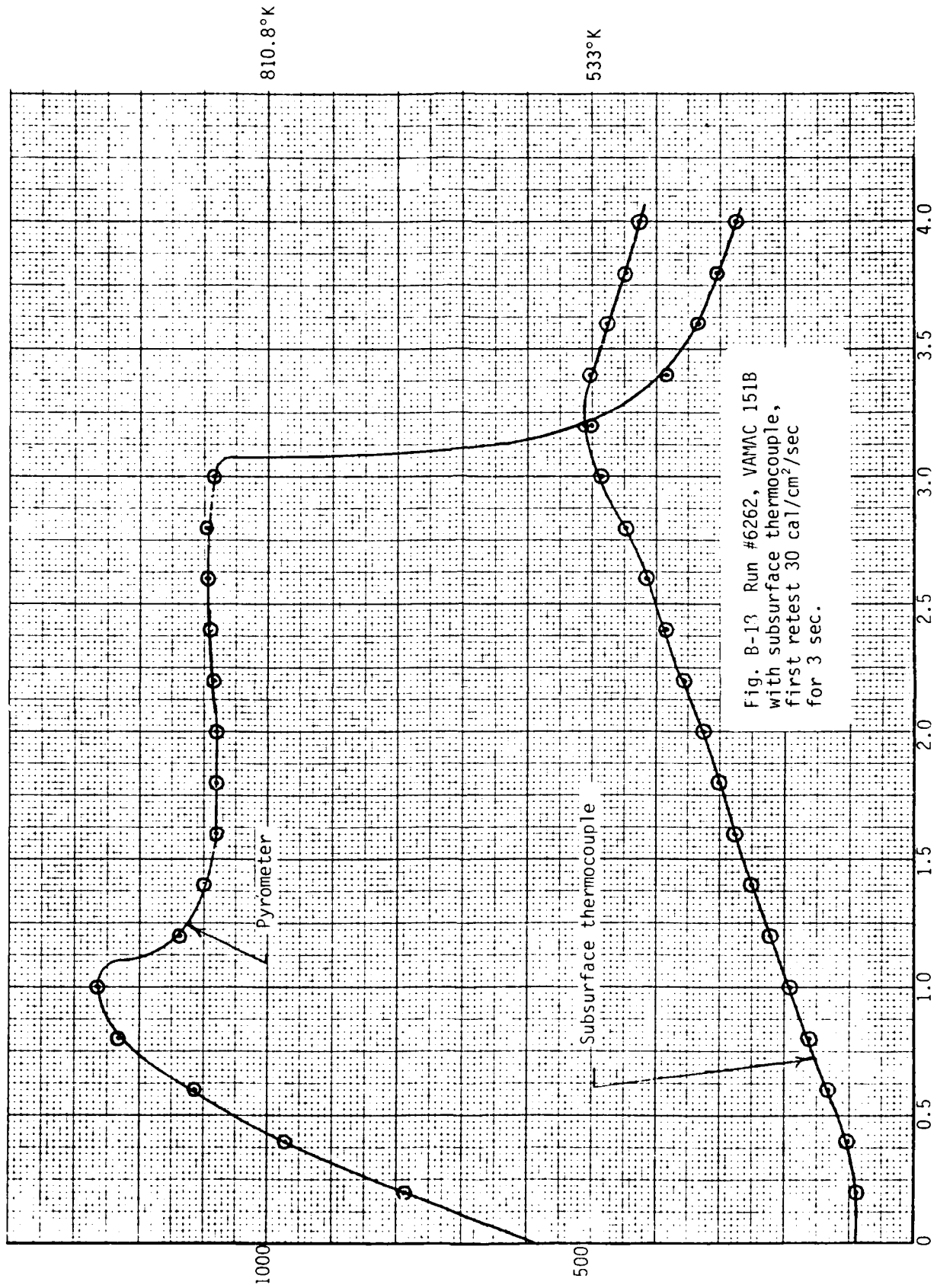


Fig. B-13 Run #6262, VAMC 151B with subsurface thermocouple, first retest 30 cal/cm<sup>2</sup>/sec for 3 sec.

Time - Seconds

810.8°K

533°K

Pyrometer

Subsurface thermocouple

1000

500

0

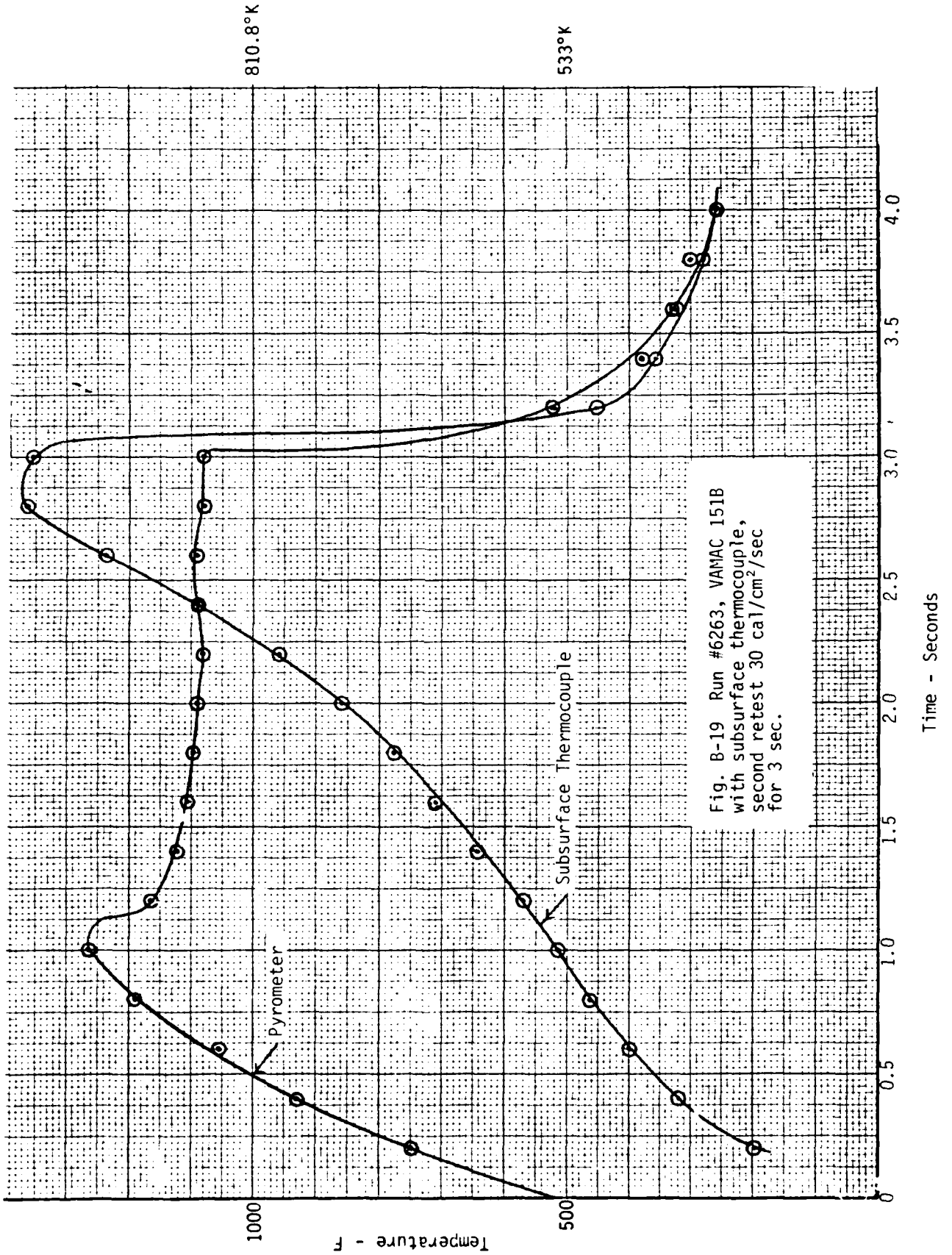


Fig. B-19 Run #6263, VAMAC 151B with subsurface thermocouple, second retest 30 cal/cm<sup>2</sup>/sec for 3 sec.

APPENDIX C  
PROPOSED TEST METHOD FOR EVALUATING THE  
THERMAL FLASH RESPONSE OF EXTERNAL PROTECTION MATERIALS  
BY UTILIZING A QUARTZ-TUNGSTEN LAMP THERMAL SOURCE

1.0 SCOPE

1.1

The purpose of this section is to describe a standard method for testing testing and evaluating the response of external protection materials to the thermal effects of nuclear weapons detonations.

1.2

This test method includes three levels of testing. These levels are:

Method A: Constant flux of  $1.6 \text{ cal/cm}^2/\text{sec}$  for 20 seconds.

Method B: Constant flux of  $30 \text{ cal/cm}^2/\text{sec}$  for three seconds.

Method C: A time variant flux equivalent to the computed net heat flux for the specific nuclear weapon threat.

1.3

Method A is intended to produce thermal diffusivity data at temperatures less than ablation temperatures. These data will be useful in supporting computer analyses of aerodynamic heating, etc.

1.4

Method B is intended to produce data pertaining to ablation characteristics of the material and can be used to support computer analysis of thermal transport during ablation.

1.5

Method C is a quality acceptance type of test and can also be used as a test of computer thermal analysis programs.

## 2.0 APPLICABLE DOCUMENTS

### 2.1 UDRI-TR-77-28 Tri-Service Thermal Radiation Test Facility

Test Procedures Handbook, May 1977, R. A. Servais, B. H. Wilt, N. J. Olson, University of Dayton Research Institute, Dayton, Ohio.

### 2.2 AFWL-TR-76-61

### 2.3 DNA 4757F

Tri-Service Thermal Flash Facility, November 30, 1978 R. A. Servais, B. H. Wilt, N. J. Olson, University of Dayton Research Inst., Dayton, Ohio.

TRAP, a Digital Computer Program for Calculating the Response of Aircraft to the Thermal Radiation from a Nuclear Explosion, October 1972, Air Force Weapons Laboratory, Kirtland AFB, New Mexico.

## 3.0 SUMMARY OF METHOD

### 3.1

This test method utilizes a quartz-tungsten lamp bank as a source. A wind stream is provided for convective cooling and smoke removal. Thermal data is taken by means of thermocouples imbedded in the test material. Calibration is via copper slug calorimeters.

## 4.0 SIGNIFICANCE AND USE

### 4.1

This method is intended primarily to gather data to support computer analyses. In addition, it can provide direct materials comparisons, and can

be used as quality control and screening type tests for materials that are required to resist exposure to the thermal environment of nuclear explosions.

## 5.0 APPARATUS

The test apparatus consists of a high density quartz-tungsten lamp bank. The lamp bank is fitted to a wind tunnel capable of MACH 0.7 or higher to simulate in flight aerodynamic effects. The lamp bank is protected from the wind stream and explosive effects from specimens by a  $\frac{1}{2}$  in. thick, minimum quartz window. The lamp bank should be capable of providing a flux uniform over a 3 x 3 in. (7.6 x 7.6 cm) area of  $60 \text{ cal/cm}^2/\text{sec}$  at the test specimen mounting position. The source is equipped with a shutter capable of opening and closing in less than 0.1 sec. Peripheral equipment consists of high speed data recorders and an analytical balance capable of resolving 0.01 gram.

Figure C-1 illustrates the test apparatus, and UDRI-TR-77-28, "Tri-Service Thermal Radiation Test Facility, Test Procedures Hand Book," describes the testing apparatus.

## 6.0 TEST SPECIMENS

### 6.1

Figure C-2 illustrates a typical test specimen configuration. The specimen is 4.0 in.  $\pm$  0.050 square (10.16  $\pm$  0.13 cm). The thickness of the specimen is optional, but must be rigid enough to resist deformation by the effects of the wind tunnel. Typically, the specimen can be supported only by its edges when mounted in the test position in a wind tunnel. A pump down tunnel such as the Tri-Service Facility at Wright-Patterson AFB creates a pressure difference of three psi forcing the specimen into the tunnel. A blow-down tunnel of appropriate dimensions will similarly produce a three psi pressure outward from the tunnel.

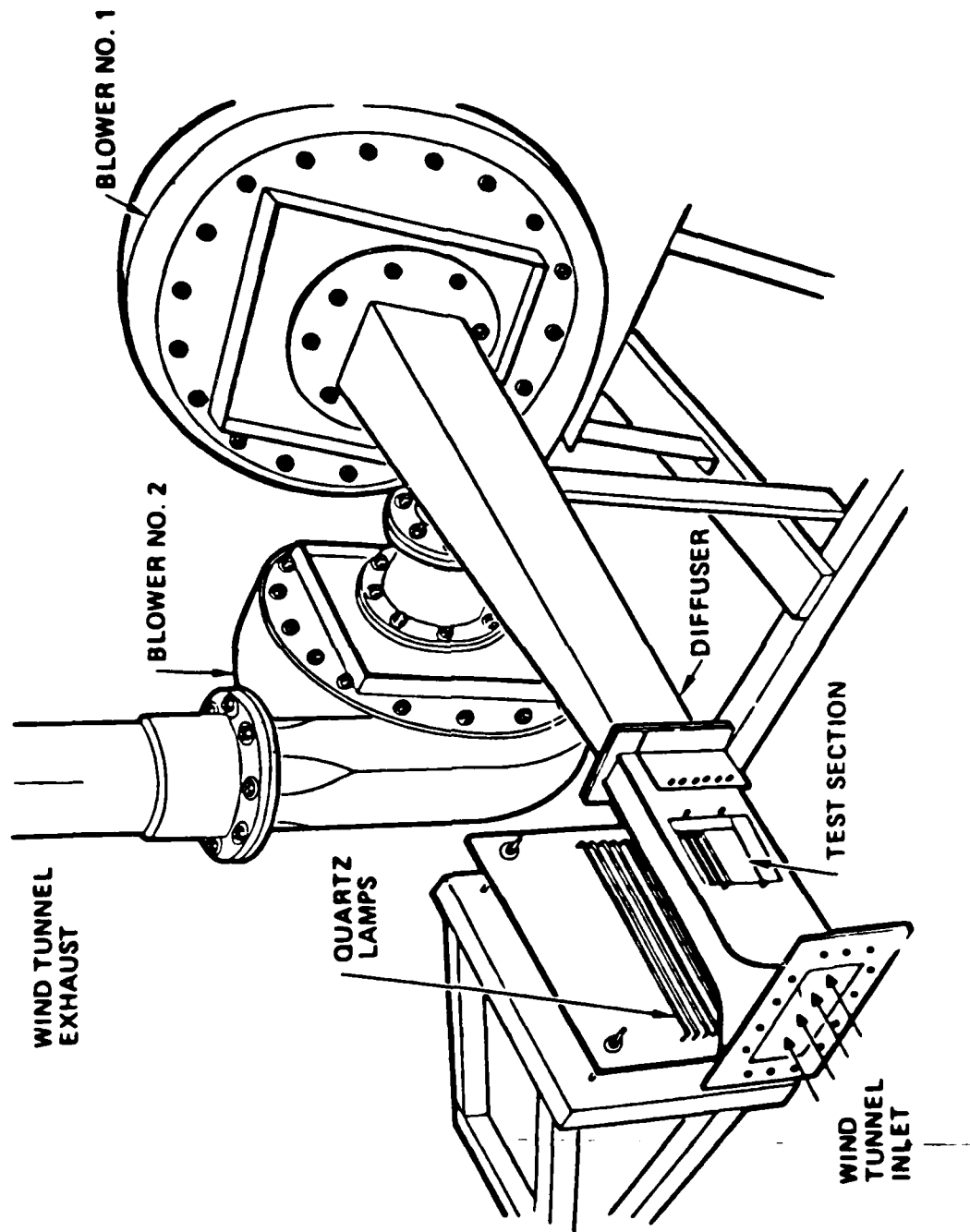
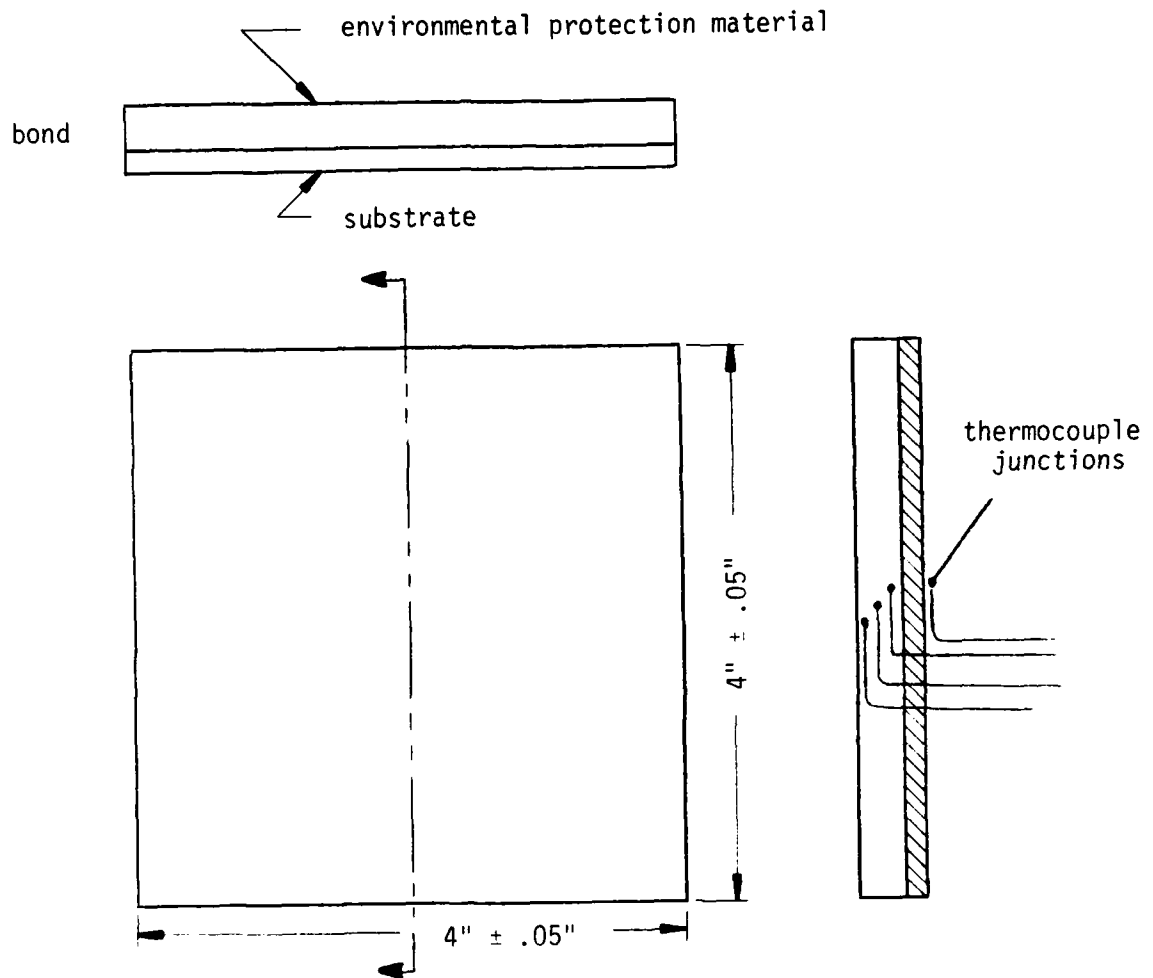


Fig. C-1 Suitable thermal flash testing facility.





- NOTES:
- (1) "t" is not to scale, typically .250"
  - (2) EPM is bonded to substrate representative of end use item with specified end item adhesive system.
  - (3) All thermocouples are parallel to the outer surface (isothermal) for 10 wire diameters, minimum.
  - (4) 1" = 2.54 cm.

Fig. C-2 Typical test specimen configuration.

## 6.2

Each specimen should be instrumented with four thermocouples. Three of the thermocouples should be imbedded in the volume of the specimen. The fourth should be mounted on the back surface of the specimen. The imbedded thermocouples should be located in an area 2 x 2 in. (5.08 x 5.08 cm) in the center of the specimen. As measured from the front surface, these thermocouples shall be placed as follows:

One thermocouple should be as close as possible to, but not penetrating the surface. A second thermocouple should be the geometric center of the environmental protection layer. The third thermocouple should be placed at the interface of the substrate and the environmental protection material.

## 6.3

The thermocouples utilized should be 0.005 in. (0.127 mm) dia. maximum, chromel/alumel. The thermocouple junctions should be welded.

## 6.4

All thermocouples should be placed so that, measured from the junction, the thermocouple wire is parallel to the front surface a distance of no less than 10 wire diameters.

## 6.5

All thermocouples should be routed such that the extension leads exit the rear surface of the specimen.

## 7. CONDITIONING

All specimens should be maintained at  $35\% \pm 15\%$  relative humidity for 48 hours minimum before testing.

## 8.0 CALIBRATION

### 8.1

The thermal flux generated by the source incident upon the test area should be measured by copper slug calorimetry. Figure C-3 illustrates a copper slug calorimeter of suitable dimensions. The front surface of the copper slug should be blackened with a suitable carbon black, such as channel black, acetylene black, or camphor black. The copper slug should be mounted in the test specimen position and exposed to a square wave pulse of the desired duration. The flux should be calculated by the following formula:

$$Q = \frac{C_1 \times t \times \Delta c \times M}{\Delta T} \quad (C-1)$$

where

$Q$  = flux, cal/cm<sup>2</sup>/sec,

$t$  = thickness in centimeters,

$\Delta^\circ\text{C}$  = temperature rise from  $T_0$  to  $T_1$ ,

$M$  = density in grams/cm<sup>2</sup>, and

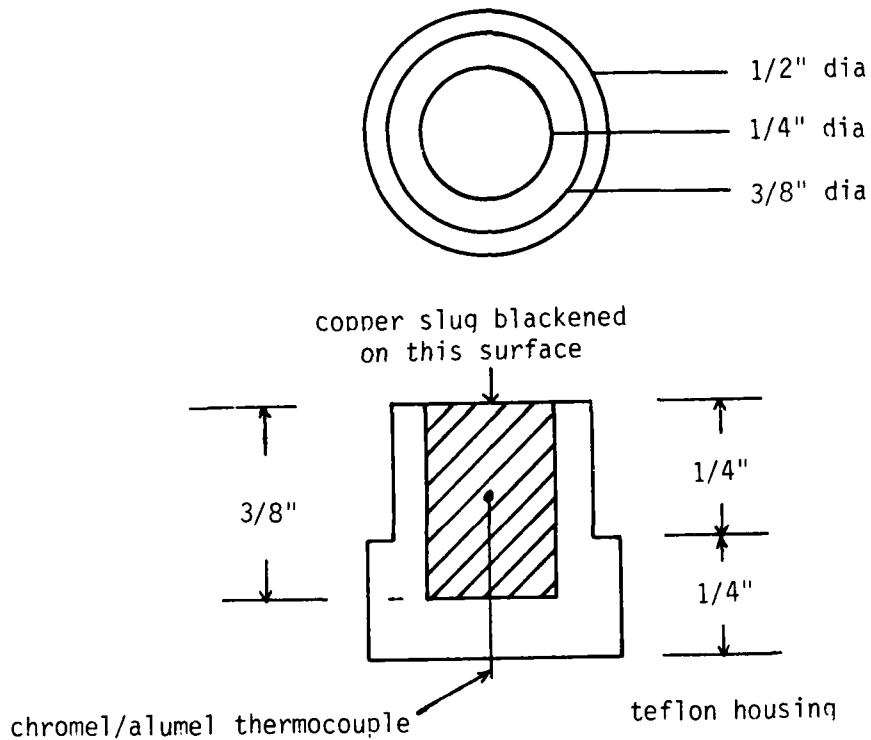
$C_1$  = specific heat of copper in cal/gm<sup>o</sup>C.

The fluence can be calculated by

$$H = C_1 \times t \times \Delta^\circ M \quad (C-2)$$

where  $\Delta^\circ\text{C}$  is the total heat rise in degrees centigrade.

For Method C, the time varying flux test method, shape of the flux curve shall be verified by use of an asymptotic calorimeter or broad band radiometer.



- NOTES:
- (1) Thermocouple is insulated except at the junction.
  - (2) Thermocouple is soldered in place in the geometric center of copper slug.
  - (3) Front surface is coated with highly absorptive black coating (0.0005" pyromark black paint, Tempil Corp., with camphor black overcoat is a suitable system).

Fig. C-3 Suitable slug calorimeter design.

## 8.2 CONVECTIVE COOLING COEFFICIENT

The convective cooling coefficient of the wind tunnel should have been thoroughly investigated and provided at the time of the test by the test facility operator.

## 8.3

The spectral reflectivity of all test specimens should be determined from 0.36 to 5.3 microns prior to thermal exposure.

## 8.4

The spectral distribution of the lamp bank should have been thoroughly characterized and provided by the test facility operator at the time of testing.

## 9. PROCEDURE

### 9.1 GENERAL PROCEDURE

All specimens should be weighed to an accuracy of  $\pm 0.01$  grams before testing. All specimens should have their thickness measured prior to testing to an accuracy of  $\pm 0.002$  in. ( $\pm 0.05$  mm) All specimens should be securely mounted in the test sample position for testing. All thermocouples should be connected to a high speed recording system. The recording system should be ice-bath referenced and capable of a full scale response in less than 0.25 seconds.

### 9.2 TEST METHOD A

The lamp bank should be adjusted to deliver  $1.6 \text{ cal/cm}^2/\text{sec}$ . The shutter should be adjusted to open for 20 seconds  $\pm 0.5$  seconds. The wind tunnel should be in operation at a nominal Mach 0.7. The specimen should be exposed at a rate of  $1.6 \text{ cal/cm}^2/\text{sec}$  for 20 seconds.

### 9.3 TEST METHOD B

The specimen should be exposed to a flux of  $30 \text{ cal/cm}^2/\text{sec}$  for 3 seconds  $\pm 0.1$  second. The wind speed should be Mach 0.7, the speed at which the best aerodynamic cooling data is available.

### 9.4 TEST METHOD C

In this method, the power to the lamp bank should be automatically controlled to net a time-varying flux at the test specimen position. The flux versus time should be based on the net computed flux of the end use item during encounter with the nuclear explosion. Such heat losses and gains as aerodynamic heating, solar heating, internal heating, surface absorptance and emittance, cloud and ground albedo, etc., should be considered in deriving the desired flux curve.

### 9.5 POST TEST MEASUREMENTS

All specimens should be weighed after testing to determine weight loss. Suitable accuracy is  $\pm 0.01$  grams.

All specimens should be measured for thickness after each test. A suitable accuracy for the measurement is  $\pm 0.002$  in. ( $\pm 0.05$  mm).

DISTRIBUTION LIST

DEPARTMENT OF DEFENSE

Defense Intelligence Agency  
ATTN: DT-2, T. Dorr  
ATTN: DT-1C

Defense Nuclear Agency  
ATTN: NATA  
ATTN: SINA  
ATTN: SPSS  
ATTN: SPTD  
ATTN: STSP  
3 cy ATTN: SPAS  
4 cy ATTN: TITL

Defense Technical Information Center  
12 cy ATTN: DD

Field Command  
Defense Nuclear Agency  
ATTN: FCTMOF  
ATTN: FCPR  
ATTN: FCTGIF  
ATTN: G. Ganong

Joint Strat Tgt Planning Staff  
ATTN: JPTM

Under Secretary of Def for Rsch & Engrg  
ATTN: Engineering Technology, J. Persh  
ATTN: Strategic & Space Sys (OS)

DEPARTMENT OF THE ARMY

BMD Advanced Technology Center  
Department of the Army  
ATTN: ATC-1, M. Capps

BMD Systems Command  
Department of the Army  
ATTN: BMDSC-1, W. Hurst

U.S. Army Material & Mechanics Rsch Ctr  
ATTN: DRXMR-HR, J. Dignam

U.S. Army Missile Command  
ATTN: DRSMI-RHB, H. Greene  
ATTN: DRSMI-RKP, W. Thomas  
ATTN: DRDMI-XS

U.S. Army Nuclear & Chemical Agency  
ATTN: Library

U.S. Army Research Office-  
ATTN: P. Radowski, Consultant

U.S. Army TRADOC Sys Analysis Actvty  
ATTN: ATAA-TDC, R. Benson

DEPARTMENT OF THE NAVY

Naval Research Laboratory  
ATTN: Code 4773, G. Cooperstein  
ATTN: Code 2627  
ATTN: Code 7908, A. Williams

Naval Sea Systems Command  
ATTN: SEA-0352, M. Kinna

DEPARTMENT OF THE NAVY (Continued)

Naval Surface Weapons Center  
ATTN: Code R06, C. Lyons

Office of Naval Research  
ATTN: Code 465

Office of the Chief of Naval Operations  
ATTN: OP 654E14, R. Blaise  
ATTN: OP 654C3, R. Piacesi  
ATTN: OP 65

Strategic Systems Project Office  
Department of the Navy  
ATTN: NSP-273  
ATTN: NSP-272  
ATTN: NSP-2722, F. Wimberly

DEPARTMENT OF THE AIR FORCE

Aeronautical Systems Division  
Air Force Systems Command  
2 cy ATTN: ASD/ENFTV, D. Ward

Air Force Aeronautical Lab  
ATTN: LLM, T. Nicholas  
ATTN: MBC, D. Schmidt

Air Force Geophysics Laboratory  
ATTN: LY, C. Touart

Air Force Rocket Propulsion Lab  
ATTN: LKCP, G. Beale

Air Force Systems Command  
ATTN: XRTO  
ATTN: SOSS

Air Force Technical Applications Ctr  
ATTN: TF

Air Force Weapons Laboratory  
Air Force Systems Command  
ATTN: DYV  
ATTN: DYV, E. Copus

Air Force Wright Aeronautical Lab  
ATTN: FXG  
ATTN: FBAC, D. Roselius

Air Force Wright Aeronautical Lab  
ATTN: MLB, G. Schmitt

Air University Library  
Department of the Air Force  
ATTN: AUL-LSE

Arnold Engrg Dev Ctr  
Air Force Systems Command  
ATTN: AEDC, AFSC/DOOP, G. Cowley

Arnold Engrg Dev Ctr  
Air Force Systems Command  
ATTN: AEDC, AFSC, Library Documents

DEPARTMENT OF THE AIR FORCE (Continued)

Ballistic Missile Office  
Air Force Systems Command  
ATTN: MNMR  
ATTN: MNRTE  
ATTN: MNN  
2 cy ATTN: MNXXH, Blankinship  
3 cy ATTN: MNXXH, J. Allen

Deputy Chief of Staff  
Operations Plans and Readiness  
Department of the Air Force  
ATTN: AFXOOS

Foreign Technology Division  
Air Force Systems Command  
ATTN: SDBG  
ATTN: TQTD  
ATTN: SDBS, J. Pumphrey

Headquarters Space Division  
Air Force Systems Command  
ATTN: AFML, G. Kirshner

Strategic Air Command  
Department of the Air Force  
ATTN: XOBM  
ATTN: DOXT  
ATTN: XPFS  
ATTN: XPQM

DEPARTMENT OF ENERGY

Department of Energy  
ATTN: OMA/RO&T

OTHER GOVERNMENT AGENCY

Central Intelligence Agency  
ATTN: OSWR/NED

DEPARTMENT OF DEFENSE CONTRACTORS

Acurex Corp  
ATTN: R. Rindal  
ATTN: C. Nardo  
ATTN: C. Powars

Aerojet Solid Propulsion Co  
ATTN: R. Steele

Aeronautical Rsch Assoc of Princeton, Inc  
ATTN: C. Donaldson

Aerospace Corp  
ATTN: H. Blaes  
ATTN: W. Barry

Aptek, Inc  
ATTN: T. Meagher

AVCO Research & Systems Group  
ATTN: W. Reinecke  
ATTN: P. Grady  
ATTN: Document Control  
ATTN: W. Broding  
ATTN: J. Gilmore  
ATTN: J. Stevens  
ATTN: A. Pallone

DEPARTMENT OF DEFENSE CONTRACTORS (Continued)

California Research & Technology, Inc  
ATTN: M. Rosenblatt  
ATTN: K. Kreyenhagen

Dupont Chemical Corp  
ATTN: F. Bailey

Effects Technology, Inc  
ATTN: R. Parisse

General Electric Co  
ATTN: C. Anderson  
ATTN: D. Edelman  
ATTN: G. Harrison

General Electric Co  
ATTN: B. Maguire  
ATTN: P. Cline

General Research Corp  
ATTN: J. Mate

Harold Rosenbaum Associates, Inc  
ATTN: G. Weber

Hercules, Inc  
ATTN: P. McAllister

Institute for Defense Analyses  
ATTN: Classified Library  
ATTN: J. Bengston

Kaman Sciences Corp  
ATTN: F. Shelton  
ATTN: J. Keith  
ATTN: J. Harper  
ATTN: D. Sachs

Kaman Tempo  
ATTN: B. Gambill  
ATTN: DASIAC

Lockheed Missiles & Space Co, Inc  
ATTN: R. Walz

Los Alamos Technical Associates, Inc  
3 cy ATTN: J. Kimmerly  
3 cy ATTN: C. Sparling  
5 cy ATTN: P. Hughes

Martin Marietta Corp  
ATTN: E. Straus

McDonnell Douglas Corp  
ATTN: L. Cohen  
ATTN: G. Johnson  
ATTN: J. Kirby

McDonnell Douglas Corp  
ATTN: M. Potter

National Academy of Sciences  
ATTN: D. Groves

Pacific-Sierra Research Corp  
ATTN: H. Brode



DEPARTMENT OF DEFENSE CONTRACTORS (Continued)

PDA Engineering  
ATTN: J. McDonald  
ATTN: M. Sherman  
ATTN: J. Dunn

Physics International Co  
ATTN: J. Shea  
ATTN: P. Spangler

R & D Associates  
ATTN: P. Rausch  
ATTN: F. Field  
ATTN: P. Haas

Rand Corp  
ATTN: R. Rapp

Rockwell International Corp  
ATTN: B. Schulkin  
ATTN: G. Perroue

Science Applications, Inc  
ATTN: W. Plows  
ATTN: J. Stoddard  
ATTN: C. Lee  
ATTN: J. Manship  
ATTN: J. Warner

Science Applications, Inc  
ATTN: W. Layson  
ATTN: J. Cockayne

Science Applications, Inc  
ATTN: A. Martellucci

DEPARTMENT OF DEFENSE CONTRACTORS (Continued)

Science Applications, Inc  
ATTN: J. Burghart

Systems, Science & Software, Inc  
ATTN: G. Gurtman

Thiokol Corp  
ATTN: J. Hinchman  
ATTN: W. Shoun

TRW Defense & Space Sys Group  
ATTN: P. Brandt  
ATTN: D. Baer  
ATTN: A. Ambrosio  
ATTN: A. Zimmerman  
ATTN: T. Mazzola  
ATTN: M. King  
ATTN: W. Wood  
ATTN: R. Bacharach  
ATTN: T. Williams  
ATTN: M. Seizew

TRW Defense & Space Sys Group  
ATTN: L. Berger  
ATTN: D. Kennedy  
ATTN: D. Glenn  
ATTN: W. Polich  
ATTN: N. Guiles  
ATTN: V. Blankinship